Transcriptome profiling of LH-producing gonadotropes in female medaka - with special emphasis on calcium-activated potassium channels

Master thesis by Line Victoria Moen

Programme for Physiology and Neurobiology

Department of Molecular Biosciences

Faculty of Mathematics and Natural Sciences

University Of Oslo

2012

TAKK!

Arbeidet i denne masteroppgaven har blitt utført på Veterinærhøgskolen, Oslo, og på IMBV ved UiO.

Først og fremst takk en stor takk til veilederne mine, Trude, Finn-Arne og Eirill. En spesiell takk til Eirill, for at du har lært meg opp på i nøyaktighetens kunst på laben, lånt meg kaffekapsler, og svart på alle mer eller mindre relevante spørsmål med et smil.

En takk rettes også til resten av forskningsgruppa på NVH og IMBV for en fin tid. Takk til Jon for hjelp til å lage alignments og fylogenetiske trær. Takk til Kristine for hjelp i innspurten av oppgaven. Takk til Kjetil for informasjon om torske-gonadotroper. Takk til Stine, Rikke og Gunnveig for hyggelige kollokvier, lunsjpauser og for å gjøre det litt lettere å være masterstudent.

Jeg vil også takke familien og vennene mine for god støtte. Takk til mamma, Knut-Arne, pappa og Toril for at dere alltid stiller opp for meg. Stor takk til Viktor og Aurora, som har korrekturlest hele oppgaven! En helt spesiell takk rettes til min aller kjæreste John André, for at du har støttet meg gjennom disse to årene og for at du alltid kommer med oppmuntrende ord når jeg trenger det.

Line Victoria Moen

Oslo, 2012

Abstract

The brain-pituitary-gonad axis regulates puberty and reproduction in all vertebrates. The two gonadotropins, FSH and LH are released from the pituitary and initiates maturing and growth of the gonads. To understand more of the changes that take place in the gonadotropes during puberty, the transcriptome of LH-producing gonadotropes from adult and juvenile medaka were profiled with high-throughput sequencing. The pituitaries were sampled from genotyped females from a (lhb:GFP) transgenic line. LH-producing cells were sorted out by FACS. RNA was isolated from the sorted cells, amplified, converted to cDNA, fragmented and sequenced with Illumina.

The sequence output from Illumina is called reads, and the reads were aligned to the medaka genome with software called TopHat. Reads were counted with the software HTSeq, and differentially expressed genes were located with the software DESeq. Some of the expressed genes that are known to be involved in reproduction, like, LHβ-subunit, GnRH-R's and dopamine receptors were focused on. The LHβ-subunit was highly expressed in both adult and juveniles. The analysis shows low expression of GnRH-R-3 in the adults. The dopamine receptors D_1, D_2 and D_3 were all expressed. Plenty of the differential expression analysis between juvenile and adult sample remains. However, the material has potential to contribute to the understanding how the gonadotropes mature.

In addition, K_{Ca} channel genes were investigated further since these channels are believed to be involved in the excitability of endocrine cells and thus important for secretion control. K_{Ca} channels were obtained from eel and cod, in addition to medaka by blasting their respective genomes with known K_{Ca} channel sequences. In eel only the BK channel, the SK1 channel and the SK2 channel sequences were obtained, while all the channel sequences were obtained from medaka and cod. The obtained sequences were analysed by sequence alignments and phylogenetic analysis, in addition to the output from RNA-seq. All K_{Ca} channels were expressed in both juvenile and female medaka, except for one variant of the SK1 channel. This particular variant of SK1 also showed a different phylogenetic relationship, than the other SK1 channels, suggesting that the channel type is non-functional. Phylogenetic analyses were performed on all the K_{Ca} channels to find the phylogenetic relationship according to species and channel type. The phylogenetic analyses showed the expected relationship according to channel type and species.

Table of content

Abbreviations

$[Ca^{2+}]_i$	cytosolic calcium concentration
APC	allophycocyanin
BK	big conductance
BLAST	Basic Local Alignment Search Tool
bp	base pairs
BPG	brain pituitary gonad
BSA	bovine serum albumin
BWT	Burrow-Wheelers transform
CaMBD	calmodulin binding domain
cDNA	complementary DNA
DAG	diacylglycerol
DNA	Deoxy ribonucleic acid
DNase	Deoxyribonuclease
E_2	estradiol-17β
EC	extracellular
EDTA:	ethylenediaminetetraacetic acid
FACS	fluoroscence activated cell sorting
FASTQ format	text-based format to store nucleotide data
FSC	forward scatter
FSH	Follicle stimulating hormone
FSH-R	FSH receptor
GFP	green fluoroscent protein
GnIH	gonadotropin-inhibitory hormone
GnRH	gonadotropin-releasing hormone
GnRH-R	gonadotropin-releasing hormone receptor
GPα	alpha- glykoprotein hormone
HTS	high-throughput sequencing
IK	Intermediate conductance
IP_3	inositol-triphosphate
kb	kilobases
Kca channels	calcium activated potassium channels
LH	luteinizing hormone
LH-R	LH receptor
mRNA	messenger RNA
Muscle	*mu*ltiple *s*equence *c*omparison by *l*og-*e*xpectation
PBS	phosphate-buffered saline
PCR	polymerase chain reaction
PD	pars distalis
PLC	phospholipase C
PPD	proximal pars distalis
q-PCR	Real-Time quantitative PCR
RCK	regulating conductance of K^+
RNA	ribonucleic acid

RNA seq	RNA sequencing
RPD	rostral pars distalis
SK	small conductance
SNP	single nucleotide polymorphism
SPIA	single primer isothermal amplification
SRY	sex-determining Y
SSC	side scatter
SSC-W	scatter pulse width
TRH	thyrotropin-releasing hormone

1 Introduction

Puberty is defined as the period when an animal acquires the ability to reproduce for the first time. The onset of puberty is marked by activation of the brain-pituitary-gonad (BPG) axis, and in teleosts as in other vertebrates, it seems like activation of the gonadotropin-releasing hormone (GnRH) system is the key event (Okuzawa 2002; Weltzien et al. 2004). Precocious puberty is a problem in many farmed fish including Atlantic cod *(Gadus morhua)* (Karlsen et al. 2006) and salmonids (McClure et al. 2007), causing reduced growth rate, reduced flesh quality and health. Additionally, uncontrolled spawning in net pens may cause genetic pollution. (For review see Taranger et al. 2010). In some other species, unfavourable environmental conditions lead to complete failure of reaching puberty in farmed fish, e.g. European eel (*Anguilla anguilla)* (Dufour et al. 2003).

What leads to the activation of the GnRH system remains to be fully identified. For the reasons mentioned above, fish is an interesting model organism in which to explore the GnRH system and other mechanisms involving the BPG axis.

1.1 The brain-pituitary-gonad (BPG) axis

The BPG axis consists of three physiologically coupled organs, which work together in a cooperated fashion and are involved in the onset of puberty and maintenance of the reproductive ability (figure 1). The BPG axis is influenced by internal and external stimuli ensuring that spawning takes place during optimal conditions. External stimuli includes photoperiod, food availability, temperature and social factors, and internal factors include neurotransmitters such as γ-amino butyric acid, neuropeptide Y, norepinephrine and kiss, in addition to numerous factors related to nutritional status such as leptin and ghrelin (Bromage et al. 2001; Levavi-Sivan et al. 2010; Schulz & Goos 1999; Taranger et al 2010)

It has been demonstrated three paralogous genes for GnRH (GnRH1, GnRH2 and GnRH3) in vertebrates. GnRH3 has only been demonstrated in teleosts. (For reviews see Okubo & Nagahama 2008; Weltzien et al 2004; Zohar et al. 2010). It is GnRH1 that is involved in the control of gonadotropin secretion (Yaron et al. 2003). The pituitary responds to GnRH by releasing follicle stimulating hormone (FSH) and luteinizing hormone (LH). FSH and LH are transported in the blood to the gonads; where they bind to receptors that upon ligand binding promote steroidgenesis and gametogenesis, making the individual capable of reproducing (Schulz & Goos 1999). The gonads secrete sex steroids that control the different stages of gametogenesis mostly together with FSH, while LH primarily regulates steroidogenesis. The sex steroids released from the gonads also regulate higher levels of the axis through various feedback mechanisms (Schulz & Goos 1999).

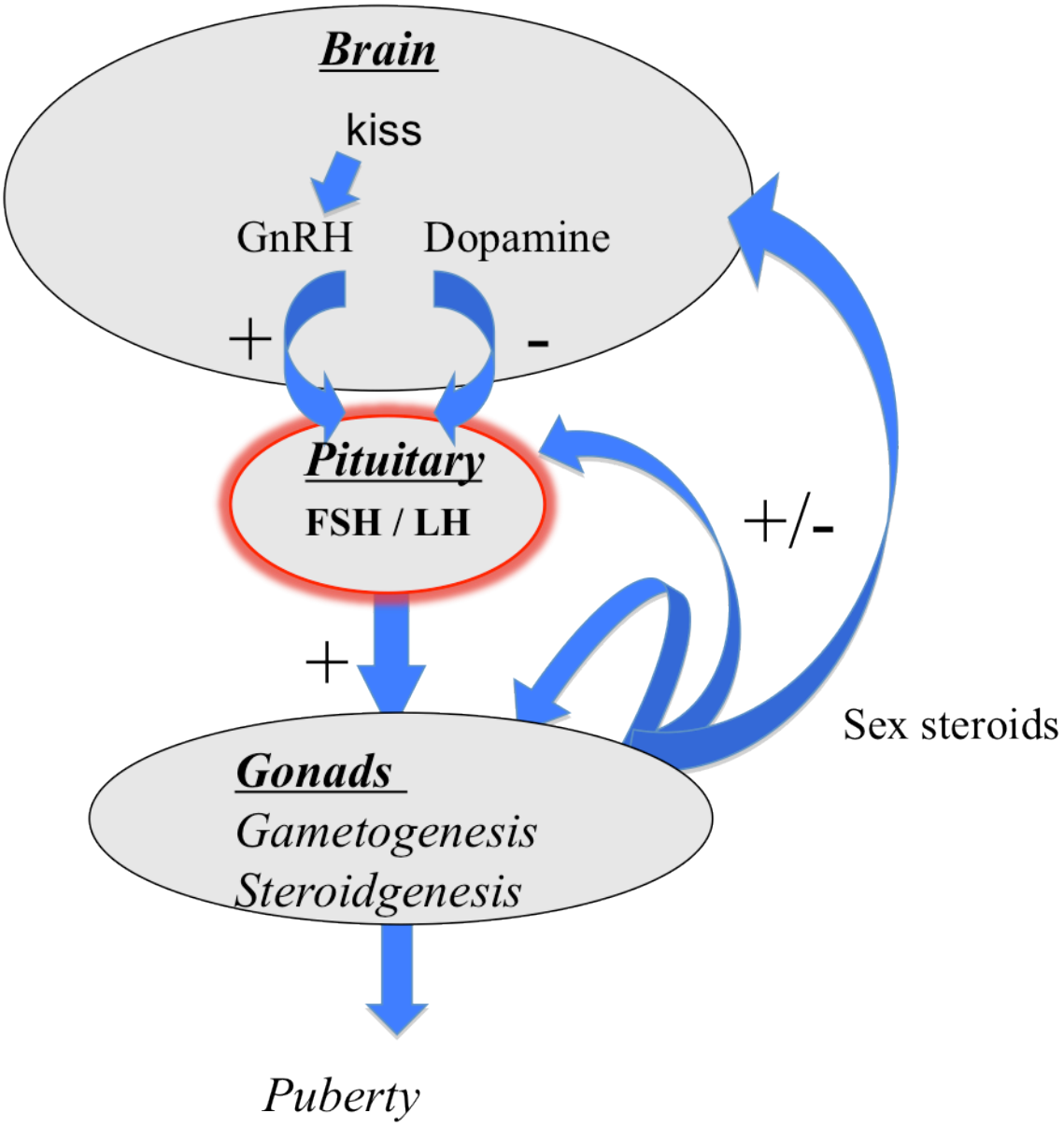

Figure 1 A simplified overview over the BPG axis. The hypothalamus (brain) secretes gonadotropin-releasing hormone (GnRH) in response to external and internal stimuli. GnRH binds to receptors and stimulates the pituitary to secrete follicle-stimulating hormone (FSH) and luteinizing hormone (LH). FSH and LH exert their effects on the gonads, leading to gametogenesis and steroidogenesis. The gonads secrete sex steroids that have positive or negative feedback effects on the BPG axis. Kiss seems to work mainly through GnRH and probably incorporates the external and internal stimuli to start puberty. Dopamine inhibits the onset of puberty in some teleost species

Kiss is secreted from kiss neurons and is cleaved into several small peptides, referred to as kisspeptins (Tena-Sempere 2006). In mammals, kiss regulates GnRH and therefore in extension gonadotropin signalling. Kiss is also involved in biological functions known to affect the BPG axis, e.g. response to photoperiodicity and nutrient level (Revel et al. 2006; Roa & Tena-Sempere 2007). Thus, in mammals kiss seem to work as a gatekeeper of puberty, and functions as a link between the internal and external factors and the BPG axis (Tena-Sempere 2006). The role of kiss has not yet been proven in teleosts. Nevertheless, two kiss genes have been identified in several species including medaka (Kanda et al. 2008; Kitahashi et al. 2009), zebrafish (*Danio rerio*) (Kitahashi et al 2009; Van Aerle et al. 2008), and fathead

minnow (*Pimephales promelas)* (Filby et al. 2008). It has been observed that kiss has a specific inhibitory effect on LHβ expression in eel (Pasquier et al. 2011).

Dopamine is a well-known inhibitor of puberty in many teleosts, and may exert its effect directly via receptors on the surface of pituitary cells, or indirectly by inhibiting GnRH neurons (Chang et al. 1990; De Leeuw et al. 1988; Vidal et al. 2004; KL Yu et al. 1991). The dopamine receptors are divided in two groups (D_1 and D_2) based on whether the receptors activate (D_1) or inhibit (D_2) the enzyme adenylyl cyclase. The dopaminergic activity varies through the reproductive cycle. (For reviews see Levavi-Sivan et al 2010; Yaron et al 2003; Zohar et al 2010). In goldfish, dopamine inhibits gonadotropin release through the D_2 receptor (Chang et al 1990). There are also indications that the gonadotropin-inhibitory hormone (GnIH) inhibits GnRH cells. GnIH is identified in birds, and inhibits steroidgenesis and development in the avian gonad. GnIH is possibly modulated by melatonin, which is involved in transmitting photoperiod information to other endocrine centres (Tsutsui et al. 2007). GnIH is present in goldfish, suggesting that GnIH is involved in teleost species as well (Sawada et al. 2002). (For review see Zohar et al 2010).

Many teleosts undergo a "dummy run" where the BPG axis seems to be fully developed the year before puberty. This is observed in striped bass *(Morone saxatilis)* (Hassin et al. 1999; Holland et al. 2001), masu salmon (*Oncorhynchus masou)* (Amano et al. 1992) and in rainbow trout *(Oncorhynchus mykiss)* (Prat et al. 1996). However, in these species the gonads are not developed enough to mature at the time of the dummy run, and thus the limiting factor may be on the gonad level (Okuzawa 2002).

1.1.1 The pituitary

As in other vertebrates, the teleost pituitary is attached to the brain with a short stalk consisting of nerve fibres. The organization of the pituitary is very similar in all vertebrates, although there exist two main morphological differences between mammals and teleosts. In teleosts the hypothalamo-pituitary portal system found in mammals is absent. Instead, the hypothalamus directly innervates the pituitary and neurohormones are released in proximity to their target cells (Kah et al. 1987; Kah et al. 1983). As a contrast to the mosaic pattern of the hormone producing cells found in mammals, the different cell types in teleosts often are clustered together in the same region (Weltzien et al 2004; Zohar et al 2010) (figure 2).

The pituitary is grossly divided into two parts in teleosts and other vertebrates, a posterior part (posterior pituitary, neurohypophysis) and an anterior part (anterior pituitary, adenohypophysis). The teleost anterior pituitary consists of *pars distalis* (PD) and *pars intermedia*. PD is divided into *rostral pars distalis* (RPD) and *proximal pars distalis* (PPD). RPD usually contains the corticotropes (secreting adrenocorticotropic hormone) and lactotropes (secreting prolactin) while PPD contains the gonadotropes (secreting gonadotropins), somatotropes (secreting growth hormone) and thyrotropes (secreting thyroid stimulating hormone). *Pars intermedia* contains melanotropes (secreting melanocyte-stimulating hormone) and somatolactotropes. Somatolactotropes secretes somatolactin, a hormone belonging to the growth hormone/prolactin superfamily that is distinct to teleosts and not found in tetrapods (Kaneko & Hirano 1993).

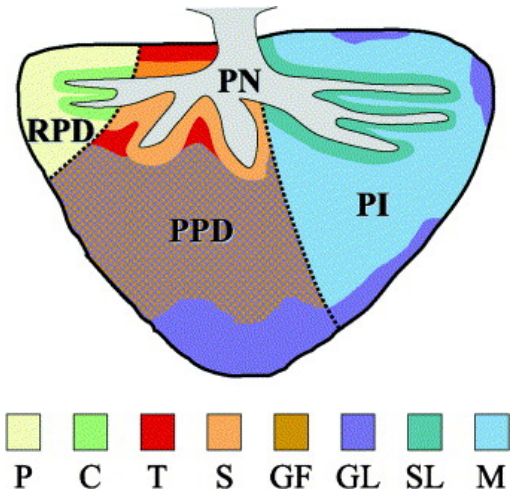

Figure 2 Sagitall view of halibut pituitary showing that the same cell type clusters in the same region. Lactotropes and corticotropes cluster in the region of RPD. In PPD the gonadotropes, somatotropes and thyrotropes are located. PI comprises clusters of somatolactotropes, melanotropes and LH-producing gonadotropes. P – lactotropes, C – corticotropes, T- thyrotropes, S – somatotropes, GF- FSH-producing gonadotropes, GL – LH-producing gonadotropes, SL- somatolactotropes, M – melanotropes, RPD – *rostral pars distalis*, PPD- *proximal pars distalis*, PI- *pars intermedia* and PN- *pars nervosa*. From Weltzien et al. (2004)

1.1.1.1 Gonadotropes: LH and FSH

In mammals both LH and FSH are produced in the same cell type. However, in teleosts, LH and FSH are produced and secreted from two different cell types. Hence teleost fish are suitable models for studying regulation and secretion of the two gonadotropins separately. Gonadotropes are as mentioned found in the PPD of the anterior pituitary, and the FSHβ- and LHβ–subunits are found throughout the PPD (figure 2). In the periphery of PI there is evidence of LH-producing gonadotropes in male halibut (*Hippoglossus hippoglossus* (Weltzien et al 2004; Weltzien et al. 2003). The two gonadotropins (LH and FSH) are heterodimeric glycoproteins consisting of a common α-subunit GPα and a distinct β-subunit that is unique for each hormone. Distinctive genes encode the subunits GPα, LHβ, and FSHβ.

The GnRH-receptor (GnRH-R) is a G-protein coupled receptor with seven transmembrane domains. Several different variants of GnRH-R are found in teleosts including rainbow trout (Madigou et al. 2000), goldfish (K.L. Yu et al. 1998), medaka (Okubo et al. 2001), Japanese eel (Okubo et al. 2000), and as many as four variants have been identified in cod (Hildahl et al. 2011). In female striped bass qPCR of GnRH-R showed that it was a significant increase in GnRH-Rs from previtellogenic fish to mature fish implying a functional role in puberty (Alok et al. 2000). GnRH directs its effects through phospholipase C (PLC). Activated PLC cleaves phosphatidylinositol-4,5-bispohsophate embedded in the membrane into inositol-triphosphate (IP_3) and diacylglycerol (DAG), both functions as intracellular second messengers. IP_3 diffuse in the cytosol and opens intracellular Ca^{2+} stores whereas DAG activates protein kinase C. Administering GnRH in goldfish increased the cytosolic Ca^{2+} ($[Ca^{2+}]_i$) levels in gonadotropes directly and activates calmodulin and protein kinase C. (For review see Chang et al. 2009).

GnRH-R upon ligand binding increases the content of the gonadotropin subunits mRNA in several teleosts. (For review see Yaron et al 2003). In common carp *(Cyprinus carpio),* the GnRH induced gonadotropin mRNA production varied across gender and phase of maturation

(Kandel-Kfir et al. 2002). GnRH injection in striped male bass induced a higher gene transcription of LHβ and GPα than of FSHβ (Hassin et al. 1998). There are several indications of a differential control over the gonadotropin subunits in teleosts; for example transcription rates of GPα, LHβ and FSHβ mRNA vary according to sex and maturity state. In most teleosts the response of GPα and LHβ transcription was similar, while the response of FSHβ was different, suggesting two different pathways of activation for these subunits. (For review see Yaron et al 2003).

1.1.2 Puberty in teleost fish

Released LH and FSH are transported in the blood from the pituitary, and eventually bind to receptors on the gonads inducing growth and maturation. There are two different gonadotropin receptors found in the gonads of teleosts, FSH receptor (FSH-R) and LH receptor (LH-R). FSH-R binds both FSH and LH, with a higher affinity for FSH, and LH-R binds only to LH. The loose control over gonadotropin binding to the FSH-R may explain that in some teleosts, LH seems to have taken over the role of FSH (Miwa et al. 1994; So et al. 2005; L. Yan et al. 1992) In tuna (*Thunnus obesus*), both FSH and LH stimulate production of estradiol-17β (E_2) and testosterone, while the response to LH is significant higher (Okada et al. 1994). The same pattern is observed in common carp, LH and FSH has similar effect in stimulating steroid secretion from the ovary, and LH being more effective than FSH (Van Der Kraak et al. 1992). However, in salmonids FSH seems more potent than LH, particularly during early stages of development, while LH comes into play in the final maturation, this is the same pattern as seen in mammals (Levavi-Sivan et al 2010). Thus, the importance of LH compared to FSH varies according to the teleosts species, sex and stage of maturation. The mature gonad releases sex steroids as E_2 in females and 11-ketotestosterone in males, which leads to maturation of the gametes (Schulz & Goos 1999). Sex steroids released from the gonads also modulate the BPG-axis through steroid feedback mechanisms (Weltzien et al 2004).

The main difference between juvenile and adult fish is that the latter produces gametes, thus enabling it to reproduce. The ability to reproduce is acquired through puberty, where the individual transforms from an immature juvenile to a mature adult. The BPG axis plays an important role and it reaches its full hormonal and gametogenetic capacity in the end of puberty (Norris 1997). The ability to reproduce is evident by the ability of spermation in males and ovulation in females.

1.2 Calcium-activated potassium (K_{Ca}) channels

Calcium-activated potassium (K_{Ca}) channels are expressed in both neuronal and non-neuronal cells (Fettiplace & Fuchs 1999; Petersen & Maruyama 1984; Vergara et al. 1998). They are involved in several physiological processes such as cell migration, proliferation, secretion, frequency tuning of hair cells and cell volume regulation, in addition to action potential frequency modulation (Ouadid-Ahidouch et al. 2000; Rohmann et al. 2009; Schwab 2001). K_{Ca} channels serve as a link between changes in intracellular concentration of Ca^{2+} and the membrane potential.

There are three subfamilies of K_{Ca} channels: big conductance K_{Ca} (BK) channels, intermediate conductance K_{Ca} (IK) channels and small conductance K_{Ca} (SK) channels. The channels are divided into subgroups based on primary amino acid sequences, pharmacological properties and single channel conduction. (For reviews see Vergara et al 1998; Wei et al. 2005).

1.2.1 Big conductance K_{Ca} (BK) channels

The α-subunit of BK channels is encoded by a single gene, KCNMA1 (also known as *slo1*) that contains several splice-sites (Rohmann et al 2009; J. Yan et al. 2008). The KCNMA1 gene is highly conserved among vertebrate species suggesting an evolutionary pressure to maintain its functions (Toro et al. 1998). BK channels contain seven transmembrane domains (S0-S6), where the N-terminal is located on the extracellular side of the membrane (figure 3a). The pore forming region is found between S5 and S6. The C-terminal side the BK channel consists of four hydrophobic (S7-S10) domains, two regulating conductance of K^+ (RCK) domains and a section of aspartic acids called "Ca^{2+} bowl" (Bao et al. 2004; Meera et al. 1997). Assembly of four KCNMA1 subunits forms the BK channel.

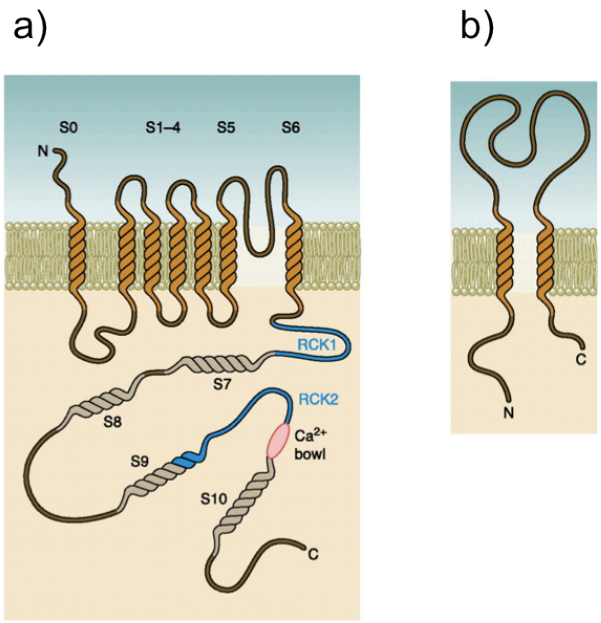

Figure 3 BK channel membrane topology. a) α-subunit consists of 7 transmembrane domains (S0-S6), the short N-terminal is extracellular and the C-terminal is intracellular. The pore region is formed between S5 and S6. The channel also has two domains regulating conductance of K^+ (RCK domains) and a calcium-bowl where calcium concentration is sensed. b) β – subunit consists of two transmembrane domains, with a short extracellular loop, both the N – and the C-terminal is on the intracellular side of the membrane. From Berkefeld et al. (2010)

Many of the BK channels associate with a β-subunit. There are four genes that code for β-subunits of BK channels (KCNMB1-4), and in vertebrate cells the majority of the BK channels are associated with a β-subunit, while no β-subunit has been found in invertebrates. The β-subunits affect Ca^{2+} sensitivity, voltage dependence and pharmacological properties (Berkefeld et al. 2006; Knaus et al. 1994; Meera et al. 2000; Orio et al. 2002). Both the C- and N-terminal of the β-subunit are located on the intracellular side of the membrane, and there are two transmembrane domains and an extracellular loop (figure 3b). Several studies have shown that E_2 in high concentrations (micromolar) binds to the β-subunit and hence

directly modulates BK channel function (Dick & Sanders 2001; Korovkina et al. 2004; Valverde et al. 1999), which indicates that BK channels are important for reproduction.

BK channels are activated both by voltage and internal Ca^{2+} and are involved in several physiological processes such as regulating smooth muscle tone, vascular tone, neuronal excitability and tuning the hair cells in cochlea (for reviews see Fettiplace & Fuchs 1999; Ledoux et al. 2006; Sah 1996; Toro et al 1998). In teleosts, evidence of the BK channels has been found by patch-clamping techniques in goby *(Gillichthys mirabilis*) (Romano et al. 1996), and by obtaining transcripts in eel (Lionetto et al. 2008) and zebrafish (Beisel et al. 2007) among others. In some teleosts, duplicate versions of the BK gene exist, reflecting the whole-genome duplication event occurring when the teleosts diverged from the tetrapod lineage (Hoegg et al. 2004; Rohmann et al 2009).

1.2.2 Small conductance K_{Ca} (SK) channels

There are three different SK channels that are encoded by the genes KCNN1-3. The exon-intron boundaries for the three channels are conserved between rat, human and mouse, which suggests a shared ancestral gene (Stocker 2004). All the SK (and IK) channels share similar membrane topology (figure 4), consisting of six transmembrane domains (S1-S6), where the pore forms between S5 and S6. N-terminal to S6, there is an intracellular calmodulin-binding domain that binds to calmodulin and helps modulate the calcium sensitivity of the SK channel, since the SK channels do not bind Ca^{2+} directly (Kim & Hoffman 2008; Schumacher et al. 2001; Wei et al 2005; Xia et al. 1998). In contrast to the BK channel, a regulatory β-subunit has not been found for the SK channel family (Vergara et al 1998).

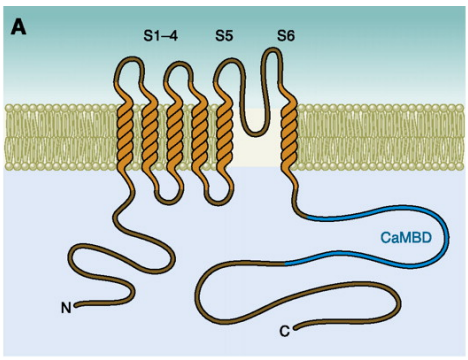

Figure 4 SK and IK channel membrane topology. SK and IK channels share the features of the membrane topology. There are six transmembrane domains (S1-S6) and the pore forms between S5 and S6. Near the C-terminal there is a calmodulin-binding domain (CaMBD) that binds to Ca^{2+} via calmodulin. From Berkefeld et al. (2010)

In mammals, SK channels are expressed in a wide range of tissues including brain, liver, heart and muscle (Köhler et al. 1996; Mongan et al. 2005; Stocker 2004). SK channels are important for the excitability for various types of excitable cells e.g. neurons, smooth muscle cells and secretory cells. SK channels are solely activated by a small elevation of $[Ca^{2+}]_i$ (Wei

et al 2005). Activation of SK channels is usually followed by hyperpolarization and thus a decrease of membrane excitability in the cell (Waring & Turgeon 2009). In the adult brain the different SK channels show an overlapping but distinctive expression, where SK1 and SK2 usually co-localize in the same area (Stocker et al. 1999; Stocker & Pedarzani 2000; Tacconi et al. 2001).

1.2.3 Intermediate conductance K_{Ca} (IK) channels

IK channels are encoded by the KCNN4 gene and have a similar membrane topology as SK channels (figure 4). It was previously thought that the IK channel was a member of the SK family, and therefore it was initially named SK4. It was renamed to IK after it was discovered that the channel had unique properties and was distinctively blocked by clotrimazol, which does not block the SK channels (Begenisich et al. 2004; Latorre et al. 1989). IK channels are without voltage or time dependence and are activated by changes in $[Ca^{2+}]_i$, and are also modulated through calmodulin. There is evidence of expression of IK channels in red blood cells, muscle and epithelia in mammals (Hoffman et al. 2003; Köhler et al 1996; Vandorpe et al. 1998). There are also indications that IK channels are involved in controlling secretion from pituitary cells (Mørk et al. 2005).

1.2.4 K_{Ca} channels in pituitary cells

Both SK and BK channels are identified in gonadotropes of mammals such as sheep, rat and mouse (Heyward et al. 1995; Kukuljan et al. 1992; Tse & Hille 1992; Waring & Turgeon 2009). In the teleost goby, pituitary cell K_{Ca} channels that resembled the mammalian BK channels were found by patch-clamping techniques (Romano et al 1996). Gene expression of both SK and IK channels has been found in the pituitary of female cod (Berg Vaule 2011). However, there is no evidence of K_{Ca} channels in goldfish gonadotropes (Van Goor et al. 1996).

In mouse gonadotropes, both SK and BK channels are important factors of secretion in response to GnRH activation. In gonadotropes pre-treated with E_2, the BK- and SK channels respond different to stimulation of GnRH compared to control cells, the SK current decreases while the BK current increases (Waring & Turgeon 2009). In rats, the composition of K_{Ca} channels varies between the different pituitary cells. The lactotropes and somatotropes express mostly BK channels, while gonadotropes express mainly SK channels (Stojilkovic et al. 2005). In cod, preliminary results from qPCR show that the LH- and FSH- gonadotropes differ in their composition of K_{Ca} channels. LH-gonadotropes express mainly SK channels, while FSH-gonadotropes express mainly BK-channels. (Hodne et al, unpublished). The cod gonadotropes also differ in their response to GnRH, where the LH-cells show a typical biphasic response (hyperpolarisation followed by increased firing frequency) and the FSH cells have a monophasic response (only increased firing frequency). The different responses could be due to the different composition of channel types (Hodne et al, unpublished). SK channels of the gonadotropes are localized in vicinity of sites of intracellular Ca^{2+} release, and therefore SK channels often regulate late hyperpolarization (Kukuljan et al 1992). In the

somatotropes, the BK channels are located near the voltage-gated Ca^{2+} -channels and respond to the accompanying changes in the $[Ca^{2+}]_i$, hence BK channels often regulate the fast after hyperpolarization (Van Goor et al. 2001). Thus, BK and SK channels may be involved in the signalling pathways of teleost gonadotropes, with different roles due to their different properties and location in the cell membrane.

IK channels, although less extensively studied than SK and BK channels, are also involved in the modulation of excitability of endocrine cells. A model system that is widely used to describe pituitary secretion mechanisms is the prolactin-secreting GH_4 cell line derived from rat anterior pituitary. Upon stimulation by thyrotropin-releasing hormone (TRH) the cells respond by changes in $[Ca^{2+}]_i$. (For review see Ozawa & Sand 1986). IK channels were recently found to be the channel type contributing most to the TRH-induced hyperpolarization in the GH_4 cells (Mørk et al 2005). In the second phase of the response to TRH, reduced activity of BK channels has been demonstrated, through currently unsolved mechanisms (Haug et al. 2004).

By patch-clamp experiments performed on unidentified pituitary cells in cod, it was evident that 30 % of the cells fire action potentials spontaneously. Additionally observations of reduced outward current following blocking of inward Ca^{2+} current with Co^{2+}, suggest that cod pituitary cells contains K_{Ca} Channels (Haug et al. 2007). Furthermore, identified gonadotropes from cod display a similar response to GnRH as the GH_4 cells show for TRH, both regarding cytosolic Ca^{2+} elevations and membrane potential changes (Hodne et al. 2012, unpublished). Together with the gene expression analysis of cod pituitary cells (Berg Vaule 2011), these findings support the hypothesis that several types of K_{Ca} channels are present in cod gonadotropes. The different responses of the different pituitary cells vary according to species and type, and the different types of pituitary cells have been show to express different composition of BK and SK channels. Thus, it is of interest to investigate the gene expression of K_{Ca} cells is in female medaka gonadotropes.

1.3 Medaka as a research model

Medaka is one of the three model organisms (medaka, European eel and Atlantic cod) that our group utilize to examine the underlying mechanisms of puberty in fish. Like other teleosts, medaka is a good model for studying gonadotrope physiology, since LH and FSH are produced in two different cell types thus making it possible to study the two gonadotropes separately. Medaka is a small Japanese rice fish that is about 3 cm long; it has short generation time and becomes sexually mature at about 2-3 months (Takeda & Shimada 2010). Medaka is a multiple spawner, and generally spawn every day. The genome of medaka is sequenced (Kasahara et al. 2007) and is available on Ensembl; the last annotation of the genome was in 2006.

Among other advantages as a research model, medaka has a sex-specific gene (DMY) that was the first non-mammalian SRY (sex-determining Y) equivalent discovered (figure 5). SRY is a sex-determining gene on the Y chromosome in marsupial and placental mammals. The DMY gene probably originated through a duplication event of an autosomal region containing DMRT1 about 10 million years ago (Kondo et al. 2009). DMY shows approximately 80 % homology with DMRT1 (Shinomiya et al. 2004; Takehana 2006). The

DMY gene thus makes medaka a preferable model organism when sex-determination is important for the project. Sex determination could be important to ensure that the intended variable is studied, and to exclude unintended sex differences between samples.

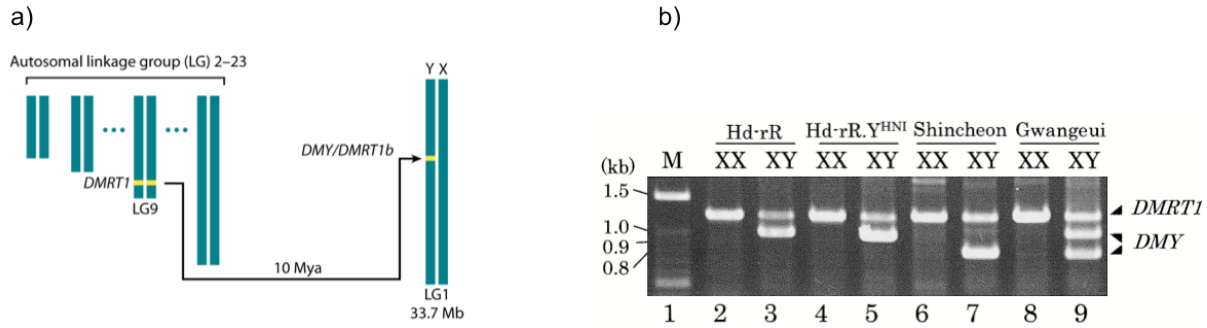

Figure 5 DMY/DMRT1 gene a) The areas marked in yellow correspond to the DMRT1 region in the autosomal linkage group and the DMY region in the sex chromosome, respectively. From Takeda et al (2010). b) DMRT 1 and DMY gene in different strains of medaka. Females with just DMRT1 band (lanes 2,4,6,8), and males with DMRT1 and DMY bands (lanes 3,5,7,9). From Shinomiya et al (2004).

Several transgenic lines for medaka exist, and our group has established a transgenic line where green fluorescent protein (GFP) is coupled to the *lhb* promoter region. Expression of GFP is convenient to sort out the LH-producing gonadotropes, to profile the transcriptomes of these cells.

1.4 RNA-sequencing

High-throughput sequencing (HTS) is parallelized sequencing, which produces enormous amount of data compared to older methods such as Sanger sequencing. E.g. one run may cover data corresponding to five human genomes. Also the elimination of the cloning step is an advantage with the HTS-technologies. (For review see Wilhelm & Landry 2009). HTS is also called next-generation sequencing, massive parallel sequencing or pyrosequencing. There are several different HTS-systems available today, and each system has to be considered before choosing the appropriate system for a project. One of the applications of HTS is RNA-sequencing (RNA-seq) which often refers to deep-sequencing of mRNA samples, but also other types of RNA could be sequenced (L. Wang et al. 2010). RNA-seq has several advantages compared to existing technologies such as microarrays. It gives researchers the opportunity to study the entire transcriptome, i.e. all the genes expressed in a given cell/tissue/organ/organism at a given time in one single run.

With RNA-seq it is possible to determine exact locations of exon-intron boundaries, and to compare differential expression between samples (Cloonan & Grimmond 2008; Mortazavi et al. 2008). Since the whole transcriptome is sequenced with RNA-seq there is a possibility of discovering novel transcripts or transcripts present in low concentration (Sendler et al. 2011). The digital nature of the RNA-reads makes it advantageous over other technologies for quantitative purposes, and it is possible to assess differences in expression of isoforms (Marguerat & Bähler 2010; Sendler et al 2011). While microarrays are restricted to using sequenced genomes, RNA-seq allows the discovery of transcriptomes of non-model organisms (Z. Wang et al. 2009). The rainbow trout brain, gonad and gill transcriptomes have

been sequenced, even though the genome of the rainbow trout has not been sequenced yet (Le Cam et al. 2012). RNA-seq is an interesting tool to explore transcriptomes, due to all additional information that could be extracted from the material. Price per base is continuously dropping, which means that more research groups can afford this technology. A lower price makes it possible to sequence parallels, instead of having non-duplicates, which is quite normal in RNA-seq and that makes the data more robust.

A typical RNA-seq experiment consists of two parts: first data generation and then data analysis (figure 6). The data generation depends on the RNA-seq technology chosen, but there are some similar features (figure 6a). RNA is isolated from the cells that are studied; possible contamination of genomic DNA is removed with DNase. Remaining RNA in the solution is converted to cDNA, and then fragmented. Adaptors necessary for amplification and sequencing are ligated to both ends of the cDNA fragments and size selection is conducted, depending on the technology. Finally the cDNA is amplified and sequenced with HTS technology, often resulting in several short reads. The cDNA fragments could be sequenced from one end resulting in single-end reads, or from both ends (stage 7, figure 6a) resulting in paired-end reads. The reads are typically 30-400 bp long, depending on the sequencing technology used.

Data analysis follows data generation and is performed by checking the raw reads. Then the data set is pre-processed by removing reads with lower quality, and artefacts of sequencing as adaptor sequences, contaminant DNA and PCR-duplications if necessary (figure 6b). The removal of the low-quality reads is not necessary, since low quality reads are less likely to align to a reference genome. However, removing them is not challenging and makes the downstream analysis faster (Wilhelm & Landry 2009). Sequencing errors could be removed to improve the overall quality of the data set. Subsequently the reads are assembled into transcripts. The assembling of transcripts could be performed by using a reference genome if it is available, by assembling the reads *de novo,* or a combination.

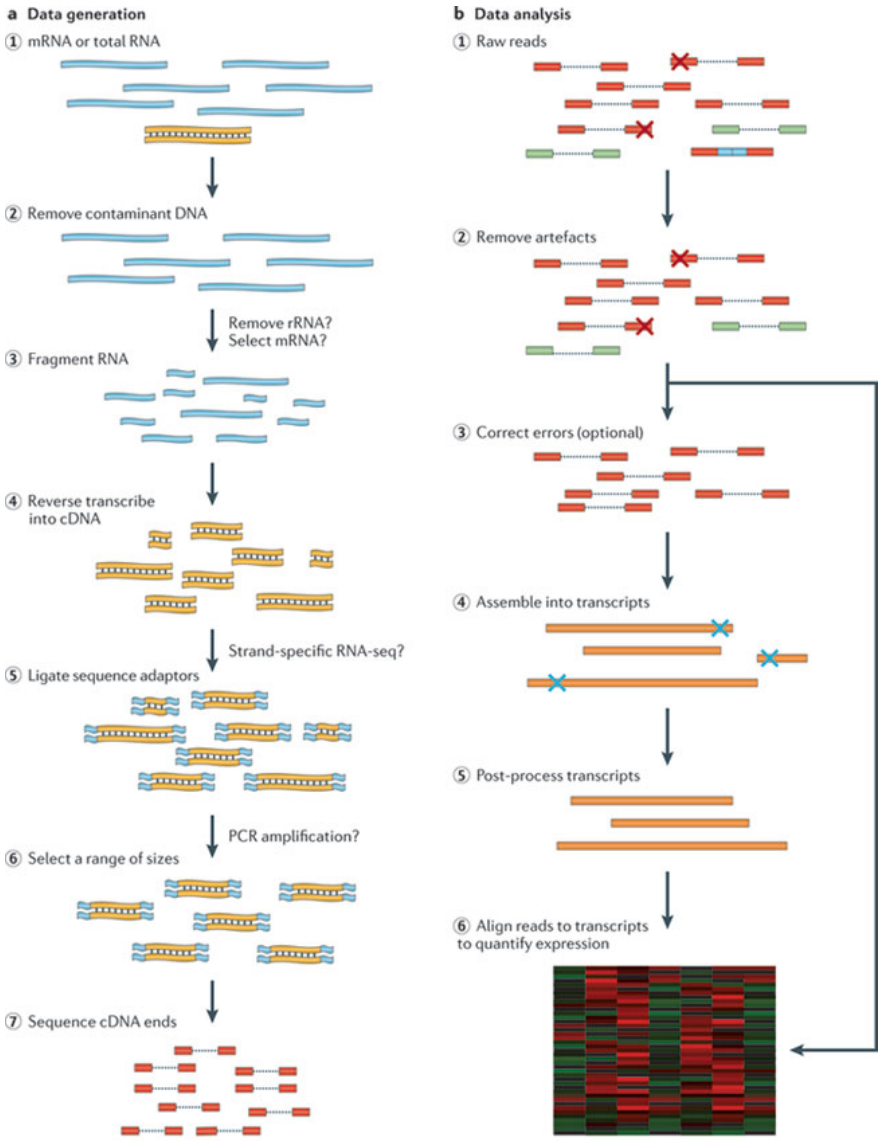

Figure 6 A typical RNA-seq experiment consists of data generation and data analysis. a) *Data generation*. To generate a RNA-seq library, RNA (blue) are extracted (stage 1), possible genomic contamination is removed from the sample using DNase (stage 2), and the remaining RNA in the sample are fragmented to fit the sequencing instrument (stage 3). The RNA fragments are reverse transcribed to cDNA (orange, stage 4) and nucleotide adaptors necessary for amplification and sequencing are ligated at each end of the fragments (stage 5) and a range of fragment size is selected (stage 6). Finally the cDNA are amplified and sequenced with high throughput sequencing technology, producing many short reads (red, stage 7). If both ends are sequenced, then paired end reads are generated, shown as dashes between the pairs. b) *Data analysis*. Following sequencing the raw reads are pre-processed by removing low-quality reads and artefacts of sequencing such as adaptor sequences (blue), contaminant DNA (green) and PCR-duplicates (stage 1 and 2). Thereafter sequencing errors could be removed (stage 3) for improvement of read quality. Thereby the pre-processed reads are assembled in transcripts (orange, stage 4). The transcripts could be further processed to remove assembly errors (blue crosses), and the transcripts are being post-processed (stage 5). Expression level of the transcripts is measured by counting of the reads that aligns to each transcript (stage 6). rRNA: ribosomal RNA, mRNA: messenger RNA. From Martin and Wang (2011).

Choosing the assembly strategy is based on whether or not there exists a reference genome, the type of data set generated, and the purpose of the sequencing study. When the transcripts are assembled, the reads are counted to find the expression level of the transcripts and possibly find differential expressed genes between samples. This is a nontrivial task, as transcripts could share exons, making it difficult to assess which read belonging to which

transcript (Martin & Wang 2011). Data analysis could be performed on several platforms and with several tools. For RNA-seq the software TopHat and Cufflinks are popular tools for differential gene and transcript analysis, however these tools require a sequenced genome (Trapnell et al. 2009; Trapnell et al. 2012).

There are currently few studies available that reports the transcriptome of pituitary cells performed with RNA-seq, even though it has been proposed that the next phase of endocrine studies would be transcriptome analyses (Carter 2006). Mostly the transcriptome of adult human, mouse and rat pituitaries have been studied, and these studies have yielded information about potentially pituitary-specific transcripts (Su et al. 2002) and different hormone-induced pathways (Wurmbach et al. 2001; Zhang et al. 2006). However, information about the transcriptome of defined pituitary cells is almost non-existent. The paired-ended strategy of RNA-seq has the ability to improve the understanding of the transcriptome, so the pituitary transcriptome should be studied more extensively with this technology (Ozsolak & Milos 2010). Our group work on the transcriptome of pituitary in European eel, collaborating with groups in Netherlands, Japan and France.

The Illumina platform is one of the providers of RNA-seq today, and is the platform that was chosen for this project. With the Illumina platform the transcriptome may be sequenced paired-end or single-end. Paired-end sequencing may improve the mapping of reads to the genome, and can offer additional information about splicing events (Ozsolak & Milos 2010).

We chose to sequence the samples of LH-producing gonadotropes from adult and juvenile female medaka with paired-end sequencing. The aim is that a snapshot of the transcriptome would reveal genes that are up –or down regulated through puberty, and that some genes may prove essential for the maturation of gonadotropes. Gaining knowledge of the type of genes that are regulated through puberty would hopefully gain more information about the maturation of gonadotropes. We especially look at K_{Ca} channels, which play an important role in the excitability of endocrine cells; these channels may be one of the factors that are regulated in puberty.

1.5 Aims of this study

By studying the transcriptome of LH- producing gonadotropes in female medaka *(Oryzias latipes),* we hope to acquire insight into which genes are involved in the functional maturation of gonadotrope cells at puberty. One important component of the signalling pathways of the gonadotropes is the calcium activated potassium ($K_{Ca)}$ channels; therefore phylogenetic analysis of these channels was conducted.

The aims of this study were to:

1) Describe the transcriptome of LH-producing cells in female medaka
2) Investigate changes in gene expression in LH-producing cells before and after puberty in female medaka
3) Perform phylogenetic analyses of calcium-activated potassium channel sequences from eel, medaka and cod obtained by data-base search

2 Materials and methods

1.1 Animal handling

The transgenic (lhb:GFP) line of Japanese medaka (d-rR strain) was kept in an indoor aquarium facility at the Department of Molecular Biosciences, University of Oslo.

The aquarium system consisted of three independent racks with water recirculation (Marine Biotech, USA). Each rack had a bio-filter, particle filter, active charcoal filter and an ultraviolet disinfection unit. To avoid build-up of nitrate, 10 % of the water was renewed daily. Production of system water was performed twice a week, and the water quality was measured before use. System water was produced by pre-filter tap water (5 and 20 µm particle filters and charcoal filter) followed by reverse osmosis. The necessary salts were added to the purified water (per 100 l): Marine salts (20 g, Seachem, Madison, USA), $CaCl_2$ (1.5 g, Merck Biosciences, NJ, USA) and $NaCO_3$ (5 g, Solvay chemicals, England). The resulting system water had a conductivity of 380 - 420 µS and a pH of 7.3 -7.8. Water quality of the racks was checked several times per week and had a conductivity of 440-490 µS and a pH of 6.8-7.5.

The fish were fed with live brine shrimps (*Artemia salina)* (Argent Chemical laboratories, Redmond, USA) and dry food (Special Diet Service, England) 4 times a day. The light regime was adjusted to 14 h light and 10 h dark and the water temperature was kept at 26 °C.

2.1 Genotyping of female medaka

Potential females were separated from the males based on phenotype. There are several secondary sex-characteristics that distinguish the male and female medaka in the d- rR strain that was used in this project (figure 7).

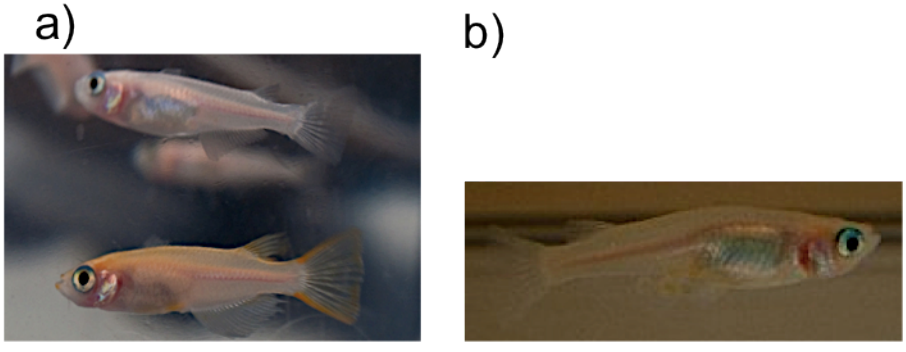

Figure 7 Female and male medaka a) The female (upper) has a white body pigmentation and the male (lower) has orange-red pigmentation. The anal fin is smooth in female and rugged in male b) Close up on female with eggs. (Photo by Eirill Ager-Wick)

Females have white body pigmentation, making it appear transparent and males have orange-red pigmentation in the d-rR strain. The female anal fin is smoother compared to the male's, that is larger and more rugged (Figure 7). Females sorted by their phenotype were anesthetized in benzocaine (0.2 – 0.5 mg/ml depending on size) before a tissue sample for genotyping was secured by clipping a piece of the caudal fin. The fin piece was placed in a mixture of 20 µl 0.5M EDTA (Invitrogen, CA, USA) and 90 µl Nuclei Lysis Solution (Promega, WI, USA) for digestion.

2.1.1 DNA isolation

The fin clip in EDTA/Nuclei Lysis Solution was homogenized using a micro pestle (Kontes Pellet Pestle Motor, Thermo Fisher scientific, USA). To digest proteins, 3 µl Proteinase K (20 mg/ml, Sigma Life Science, USA) was added and the solution was incubated at 55 ºC for 30 min. The sample was cooled down to room temperature for 5 min. To precipitate the remaining protein in the sample, 33 µl Protein Precipitation Solution (Promega) was added and the solution vortexed for 20 s and subsequently incubated on ice for 5 min and centrifuged at 4 ºC for 4 min at 16 000 g. The supernatant was collected and transferred to a new Eppendorf tube with 100 µl isopropanol to precipitate the DNA. To make the DNA pellet visible, 1 µl of GlycoBlue (150 µg/ml, Ambion, Austin, TX, USA) was also mixed in, and the sample centrifuged at 4 ºC for 4 min at 16 000 g. The supernatant was removed and 100 µl of 70 % ethanol was added to wash the pellet, and subsequently the tube was centrifuged at 4 ºC for 4 min at 16 000 g. Ethanol was carefully removed from the pellet. The pellet was left to dry a few min to let the ethanol evaporate completely, and then resuspended in 10 µl DNA Rehydration Solution (Promega) at 55 ºC for 30 min, and used in a PCR reaction immediately.

2.1.2 PCR for sex-specific gene

The medaka fin clips were genotyped by a touchdown PCR. The same pair of primers amplified the somatic DMRT1 gene and the male-specific DMY gene (forward 5'-CCGGGTGCCCAAGTGCTCCCGCTG-3' and reverse 5'-GATCGTCCCTCCACAGAGAAGAGA-3'). The two genes were PCR- amplified in a mix of $MgCl_2$ (50 mM), 10X PCR buffer minus $MgCl_2$ (both from Invitrogen), dNTP mix (10mM, Clontech, CA, USA), Platinum *Taq* DNA Polymerase (1U, Invitrogen), forward and reverse primer (10pmol each, Eurofins MWG Operon, Germany).

An initial denaturing step for 2 min at 94 ºC was followed by 10 cycles comprising denaturation for 15 s at 94 ºC, annealing for 15 s where the temperature dropped one degree centigrade per cycle from 63-53 ºC and extension for 70 s at 72 ºC. This was followed by 30 cycles comprising 15 s at 94 ºC, 15 s at 53 ºC and 70 s at 72 ºC. The program was completed with a final elongation step for 5 min at 72 ºC.

To verify that the sampled fish were females, the PCR product was loaded on a 1 % agarose gel stained with SYBR Safe DNA gel stain (Invitrogen) in order to visualize nucleic acids. Before loading, load dye (Invitrogen) was added to the PCR product. A female positive and a male control sample were also loaded on the gel, together with 1 kb ladder (Promega). Since

the male and the female fish should both have the DMRT1 gene, the male control was added to confirm that both bands (DMY and DRMT1) were amplified. Electrophoresis was conducted using an electrical field of 80 V for approximately 30 min.

2.2 Dissection and dissociation

2.2.1 Pituitary dissection

Medaka extracellular (EC) medium was made by dissolving salts (134 mM NaCl (VWR, USA) 2.9 mM KCl (Sigma), 2.1 mM $CaCl_2$ (Merck Biosciences), 1.2 mM $MgCl_2$ (Fluka, USA)), sugar (1.8 mM glucose (Fluka)), buffer (10 mM HEPES, Sigma) and protein (1 % BSA (Bovine serum albumin, Sigma)) in water. Thereby pH was adjusted to 7.75 using NaOH and the osmolality (number of osmoles per kilograms of solvent) adjusted to 280 mOsm/kg with NaCl. The medium was millipore filtered before use. The pH and osmolality of the phosphate-buffered saline (PBS; Invitrogen) used in cell dissociation were similarly adjusted to 7.75 and 280 mOsm/kg each.

The genotyped females were anaesthetized in benzocaine (0.2 - 0.5 mg/ml depending on size) in system water prior to dissection. The fish was pinned to a wax plate, the roof of the skull removed using fine tweezers and the spinal cord quickly severed (figure 8). The brain was flipped over to expose the pituitary, and the pituitary removed and placed in EC medium in an Eppendorf tube on ice.

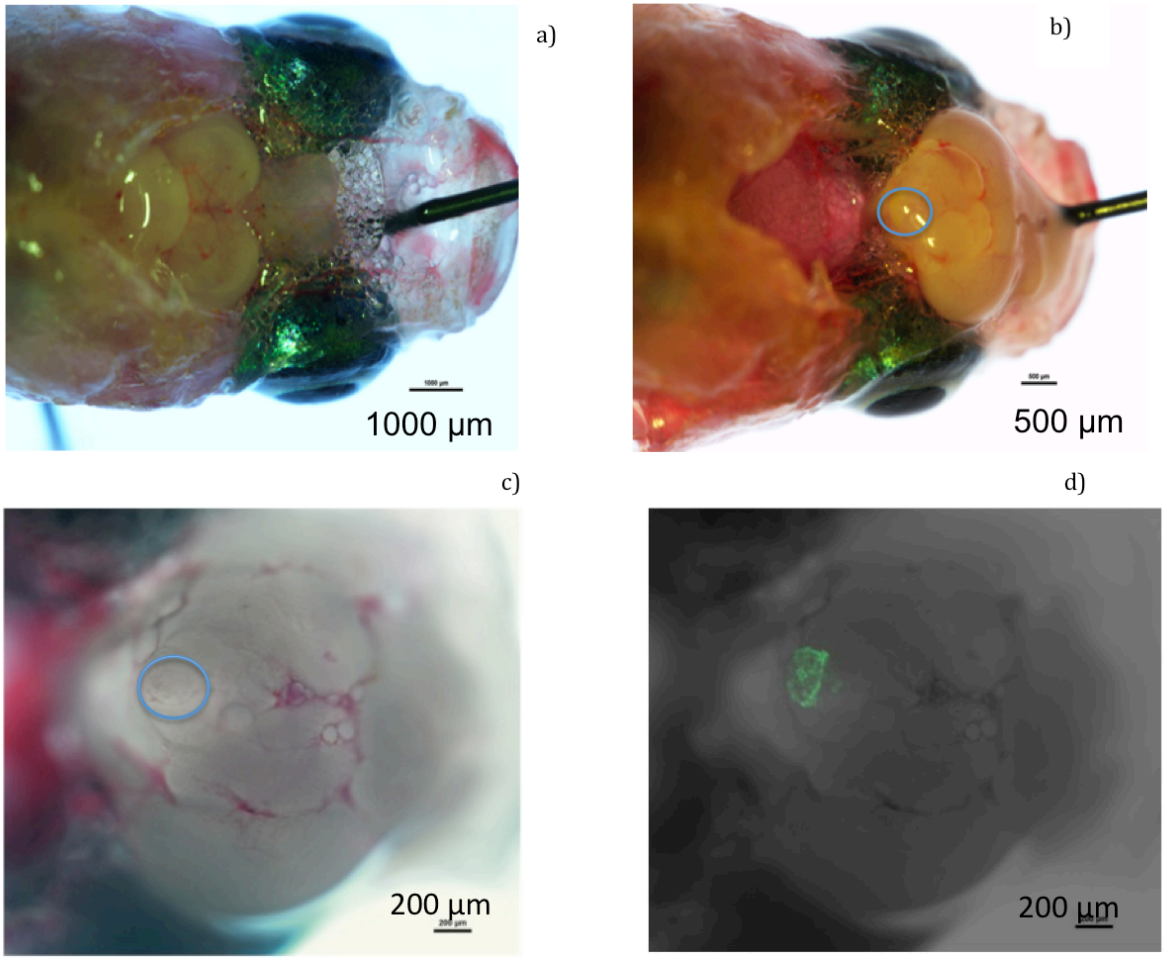

Figure 8 Pituitary dissection a) Anaesthetized medaka with roof of skull removed to expose the brain. b) The brain is flipped over; the pituitary is marked by the blue circle. c) Close-up photo of the pituitary, the pituitary is marked by the blue circle. d) Fluoroscent image of c) showing GFP-expression in the pituitary (photos by Eirill Ager-Wick (c+d)).

2.2.2 Cell dissociation

The tissue sample (containing the pituitaries) was centrifuged briefly on a table top centrifuge (Galaxy MiniStar, VWR), the EC medium was removed and replaced with 0.1 % trypsin (Sigma, USA) and 0.2 % collagenase (Merck Biosciences) dissolved in PBS to wash the pituitaries. The tissue sample was centrifuged again, and the trypsin/collagenase solution removed and replaced with 1 ml fresh trypsin/collagenase solution and incubated in a shaking water bath (Julabo SW22, Julabo, USA) at 26 ºC for 30 min to dissociate the cells. The tissue sample was then centrifuged and the trypsin/collagenase solution replaced with 0.1 % trypsin inhibitor (Sigma) and about 2.5 µg/ml deoxyribonuclease (DNase, Sigma) in PBS. Subsequently the sample was incubated in the shaking water bath at 26 ºC for 20 min to stop the chemical dissociation. The tissue sample was centrifuged again and the trypsin inhibitor solution removed and replaced with ice-cold PBS.

Then the tissue sample was mechanically dissociated on ice by repeated pipetting with a glass pipette. The resulting cell suspension was centrifuged at 4 ºC for 10 min at 200 g. To remove small particles/loose GFP fragments that could interfere with the FACS sorting, the supernatant was removed with a vacuum glass pipette. The pellet was resuspended in 100 µl

EC medium, and allophycocyanin (APC) Annexin V (BD Pharmingen, USA) added to the solution to mark the apoptotic cells. APC Annexin V binds to the membrane phospholipid phosphatidylserine, which is flipped to the outside of the membrane in apoptotic cells (figure 9). The solution was mixed and left on ice until the FACS sorting was performed later the same day. The fluorophore APC was chosen because its fluorescence spectrum does not overlap the fluorescence spectrum of GFP.

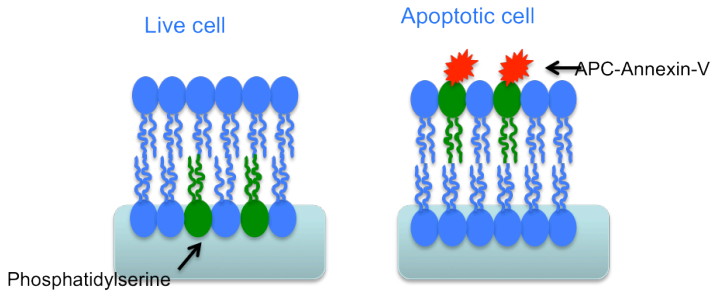

Figure 9 Staining with APC Annexin V. APC Annexin V binds to Phosphatidylserine that is flipped on the outside of the membrane in an apoptotic cell. (Made in Powerpoint based on a figure from www.biomol.de).

2.3 FACS sorting

GFP- expressing LH-producing gonadotropes from juvenile and adult medaka were sorted out by fluorescence activated cell sorting (FACS). The FACS instrument is a specialized type of flow cytometer (figure 10). It provides a method for sorting a cell suspension marked with fluorophores into different containers based on size and fluorescent characteristics of the individual cells (Ibrahim & van den Engh 2007).

The cell suspension is compressed by gas to form a fluid where the cells emerge one after another. The laser will then illuminate only one cell at any given time. Detectors measure the light scatter from the laser; the forward scatter (FSC) indicates the size of the cell and the side scatter (SSC) indicates the granularity or fluorescent character of the cell. Subsequently the cell suspension is distorted into droplets by a vibration mechanism. The system is adjusted so that it is a high probability for each droplet to contain only one cell. An electrical charge ring is placed just after the fluid is broken into droplets. The particles will be given a charge according to their fluorescence and size. The charge determines which of the sorting tubes the particle is sorted in.

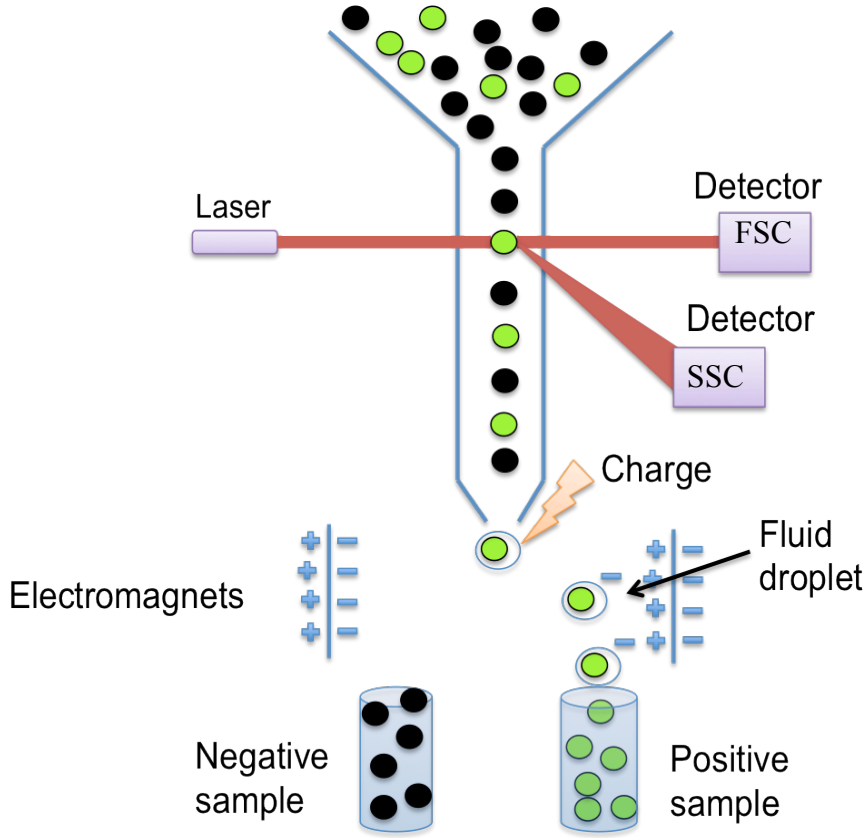

Figure 10 FACS sorting The cell suspension is pressured by gas through the nozzle, where they emerge in a single file. The diameter is smaller at the end, which makes the cells move faster and causing the cells to have a greater distance to each other near the end. The laser beam illuminates one cell at any given time and detectors measure the light scatter. The forward scatter (FSC) measures the size of the cell, while the side scatter (SSC) is dependent on the granularity or the fluorescence of the cell. The fluid is broken into droplets by a vibration mechanism and then the particles are given a charge according to the scattering angle measured. (Figure made in PowerPoint, based on Sabban, 2011)

2.3.1 Procedure of FACS

Before the samples were sorted on the FACS instrument (BD FACS Aria Cell Sorter, BD Biosciences USA) the accuracy of the equipment was tested and adjusted to the samples, consequently some material (including positive cells) was lost. To minimize the damage on the cells when collected into the sorting tube, a small volume of EC solution was added to the bottom of each tube. Prior to FACS the cell suspension was filtered through a 70 µM filter to remove cell-clusters, which could clog the instrument. The GFP-positive and APC-negative (i.e. non-apoptotic *lhb*-expressing) cells were collected at 4 ºC. The cells were then centrifuged for 10 min at 200 g, before being lysed in 300 µl of Trizol (Invitrogen) during vortexing for 1 min and finally snap frozen in liquid nitrogen. The sample was stored at -80 ºC until RNA isolation.

2.4 RNA isolation

The homogenized cells (in 300 µl Trizol) were thawed at room temperature. Additionally 200 µl Trizol were added to the sample, because previous testing had showed that the yield was

higher when isolating in 500 µl Trizol. The sample was mixed and incubated at room temperature for 5 min. To phase separate the solution, 100 µl chloroform was added to the sample. The sample was vortexed and incubated at room temperature for 3 min, before being centrifuged at 4 ºC for 15 min at 14000 g. The sample was separated in 3 phases; one upper aqueous phase where the RNA remained, an interphase and a lower organic phase. About 2/3 of the upper phase was harvested and transferred to a new tube. The RNA in the sample was precipitated with 250 µl isopropanol, and 1 µl GlycoBlue (60 µg/ml) added to the sample to make the small pellet visible. The sample was incubated at – 20 ºC for minimum 10 min and then centrifuged at 4 ºC for 10 min at 14000 g. After removing the supernatant, the pellet was washed with 500 µl ice-cold 75 % ethanol and centrifuged at 4 ºC for 5 min at 5000 g. The 75 % ethanol was removed, and the pellet briefly air-dried. The pellet was resuspended in 10 µl of RNase free water and incubated at 55 ºC for 10 min to dissolve the pellet. The dissolved RNA was then stored at -80 ºC until cDNA synthesis and amplification.

RNA quality and degree of degradation was measured with Qubit 2.0 Fluorometer (Invitrogen) and Bioanalyzer (Agilent Technologies, USA) respectively. Qubit is a precise and sensitive method for measuring DNA and RNA concentrations as low as 10 pg/ µl. The Agilent 2100 Bioanalyzer and Agilent RNA 6000 Pico Kit were used to measure the RNA-quality. The RNA quality is measured as the ratio between 18S and 28S ribosomal units, given as a RIN (RNA integrity number) that ranges from 1 (totally degraded RNA) to 10 (intact RNA). The RIN value has to be at least 7 for reliable RNA-sequencing. In our samples the RIN values ranged from 7.2 to 8.2.

2.5 cDNA synthesis and amplification

Due to the small amount of RNA extracted, the RNA was amplified before RNA sequencing (RNA seq) to have sufficient template. This was carried out by use of the Ovation RNA Seq System V2 kit (NuGEN, CA, USA).

To remove potential traces of genomic DNA in the sample, the RNA was DNase-treated (TURBO DNA-free, Ambion) following the procedure from the manufacturer. The cDNA synthesis and amplification was carried out on a PCR-plate, to ensure stability later in the process, were the use of a ring magnet (Beckman Coulter, USA) was necessary. The first and second strand cDNA synthesis was performed on ice.

Primer annealing was performed by adding 2 µl of First Strand Primer Mix (NuGEN) and 5 µl of isolated RNA in each well followed by mixing with a pipette. The PCR-plate was incubated in a thermal cycler at 65 ºC for 5 min. Thereby first strand synthesis was performed by adding 2.5 µl of First Strand Buffer Mix (NuGEN) and 0.5 µl of First Strand Enzyme Mix (NuGEN) to each well and then mixing with a pipette. First strand cDNA synthesis (reverse transcriptase) was carried out by incubation in a thermal cycler at 4 °C for 1 min, at 25 °C for 10 min, at 42 °C for 10 min and finally at 70 °C for 15 min. The PCR-plate was briefly centrifuged to collect condensation in the wells.

When first strand cDNA synthesis was completed, second strand cDNA synthesis was started immediately by adding 9.7 µl of Second Strand Buffer Mix (NuGEN) and 0.3 µl of Second Strand Enzyme Mix (NuGEN) to each well. The content of each well was mixed with a pipette and the PCR-plate incubated at 4 °C for 1 min, 25 °C for 10 min, 50 °C for 30 min and

finally at 80 °C for 20 min. The PCR-plate was briefly centrifuged again, to collect condensation in the wells.

The cDNA was purified at room temperature using the Agencourt RNAClean XP beads (from Beckman Coulter and provided with the NuGEN kit) (figure 11). Thirty-two µl of the bead suspension was added to each well and mixed well. The PCR-plate was incubated for 10 min at room temperature to let the cDNA molecules attach to the magnetic beads. The PCR-plate was then transferred to a ring magnet and incubated for 5 min to clear the solution of the magnetic beads (with cDNA attached). Keeping the PCR-plate on the magnet, 45 µl of the supernatant containing possible contaminants was removed from each well. Some of the volume was left behind to minimize loss of beads (and cDNA). The beads with cDNA attached were washed by adding 200 µl freshly prepared 70% ethanol to each well. Following incubation on the magnet for 30 s, the ethanol was removed. This washing procedure was repeated twice. The beads were left to air-dry on the magnet for 15-20 min. It was critical that all the ethanol had evaporated before continuing the procedure.

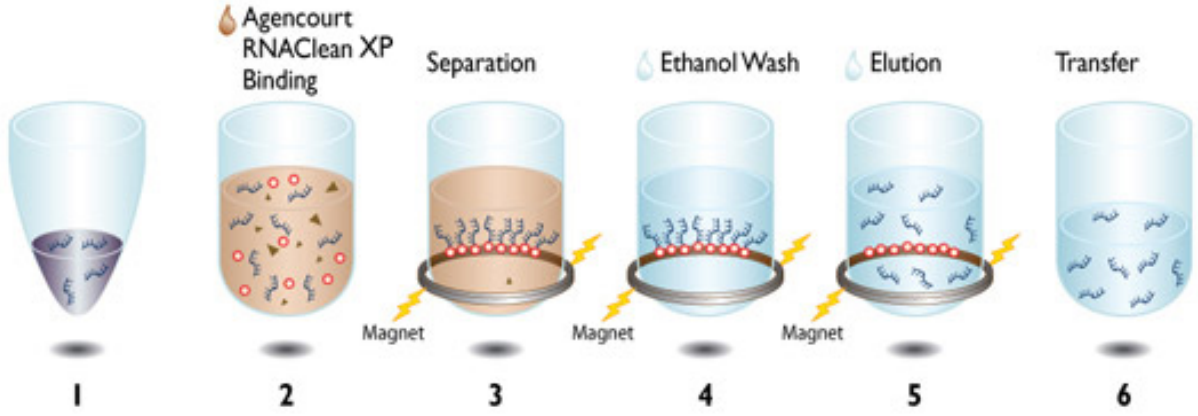

Figure 11 cDNA purification performed on a ring magnet 1. cDNA synthesis from the sampled RNA as described in the text. 2. Binding of cDNA-molecules to the magnetic beads to purify the cDNA. 3. The magnetic beads (with cDNA attached) were attracted to the magnet. The supernatant containing possible contamination was removed and the cDNA remained bound to the magnetic beads. 4. The bound cDNA was washed with ethanol. Then the PCR-plate was removed from the magnet for amplification of cDNA. 5. After amplification, the cDNA was eluted on the magnet. The cDNA was no longer attached to the beads. The cDNA remained in the solution while the beads were attracted to the magnet. 6. Transfer of the cDNA into a new well. (From Beckman Coulter, Inc.)

The PCR-plate was removed from the magnet with the cDNA still bound to the beads, and SPIA (Single Primer Isothermal Amplification) amplification started. To elute and amplify the cDNA 20 µl of SPIA Buffer Mix, 10 µl SPIA Primer Mix and 10 µl SPIA Enzyme Mix was added to each well and thoroughly mixed with a pipette. The majority of the beads were at that time in the solution. The PCR-plate was incubated at 4 °C for 1 min, at 47 °C for 60 min and at 80 °C for 20 min to amplify and elute the cDNA from the beads. The PCR-plate was briefly centrifuged to collect condensation in the wells, and then transferred to the magnet and incubated for 5 min to remove the beads, and leave the cDNA in the solution. The supernatant containing the amplified cDNA was transferred to a new tube.

2.5.1 Purification of cDNA

QIAGEN MinElute Reaction Cleanup Kit was used to clean up the cDNA. All the centrifugation steps were carried out at 12 000 g at room temperature.

The entire volume of cDNA was added to 300 µl of Buffer ERC (QIAGEN) in an Eppendorf tube, then the sample was vortexed for 5 s and centrifuged briefly. The sample was loaded on a MinElute column (QIAGEN) placed in an Eppendorf tube, then centrifuged for 1 min, before the flow-through was discarded. To each column, 750 µl of Buffer PE (QIAGEN) was added and then centrifuged for 1 min to wash the cDNA. The flow-through was discarded, and the column placed in the same Eppendorf tube and centrifuged additionally 2 min, to remove all traces of Buffer PE. After discarding the flow-trough again, the column was placed in a new Eppendorf tube. To elute the cDNA, 22 µl of Buffer EB (QIAGEN) was added to the centre of the column. Incubation of the column for 60 s was followed by centrifugation for another 60 s and the flow-through collected. The yield of the purified cDNA was measured on NanoDrop spectrophotometer (NanoDrop, Thermo Fisher scientific). The cDNA was stored at -20 °C until RNA-sequencing.

2.6 RNA sequencing

RNA-seq is performed by converting RNA to cDNA, making a cDNA library that meet the requirement of the RNA-seq instrument, amplifying the cDNA library, sequencing the library and finally analysing the sequencing output. The sequencing service was provided by the Norwegian Sequencing Centre (www.sequencing.uio.no), a national technology platform hosted by the University of Oslo and supported by the "Functional Genomics" and "Infrastructure" programs of the Research Council of Norway and the Southeastern Regional Health Authorities.

2.6.1 Data generation

The RNA-seq was performed on a HiSeq2000 (Illumina, USA). First, a sequencing cDNA-library specific for HiSeq2000 was made by fragmenting the amplified cDNA. By gel filtration, fragments in the range of 200 – 600 bp were selected. Nucleotide adaptors necessary for amplification and sequencing were ligated to both ends of the cDNA-fragments (figure 12a). The cDNA molecules were pumped in low concentrations onto a glass slide, where complementary primers were attached. The adaptors of the fragments were then hybridized to the primers, thereby making the cDNA-library attach to the glass-plate. Several rounds of PCR amplified the library. This process is called bridge amplification and generated several clusters with identical cDNA- molecules in each cluster (figure 12b).

The clusters of cDNA were copied base-by-base using the four nucleotides (ACGT) (figure 12c). Each nucleotide had a unique fluorescent label that also functioned as a block for incorporation of the next nucleotide. After each synthesis step, the clusters were excited by a laser, which caused a fluorescent signal from the label attached to the last incorporated base. Further, the fluorescence label was removed by enzymatic cleavage, allowing the addition of

the next base. A built-in camera captured the fluorescent signal after each incorporation step. The time-series of images made up the sequence and was later converted to FASTQ format.

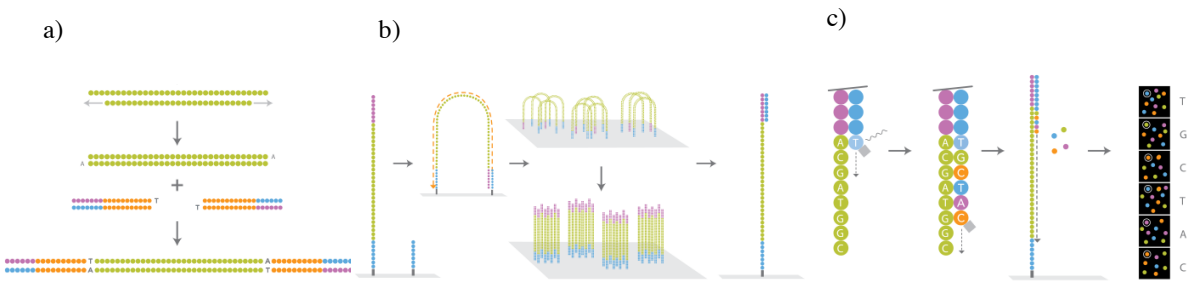

Figure 12 Data generation. a) Ligation of primers to each end of individual cDNA molecules (library preparation). b) The library is hybridized to primers that are attached to the glass slide where the library is amplified. The amplification process is called bridge amplification due to the bending of the DNA-molecules. The amplification results in clusters of cDNA, where the cDNA molecules in each cluster are identical. c) The fluorescent signal of the four, labelled nucleotides is captured by a built in camera. The fluorescent marker works as a block for incorporation of a new base and is removed before the next base is incorporated. The time-series of images is translated to a sequence (figures by Illumina inc).

The FASTQ format is a text-based format to store nucleotide data, with quality scores included for each base. The cDNA molecules could be sequenced from one end producing single-end reads, or sequenced from both ends producing paired-end reads. In this project the sequenced data comprised of 68 535 934 and 81 119 072 paired-end reads (each read 100 bp long) from juveniles and adults, respectively. These reads contain all the information about the transcriptome and thus the genes that were expressed at sampling time.

2.6.2 Sequence analysis

After sequencing the cDNA library, the FASTQ file that contained the sequenced reads was examined. Each sequenced base had a quality score, which is a score based upon the probability of that base being sequenced correctly (compared to the template). It is critical to check the data amount to know how much data there is to handle and to check the data quality to know if the RNA-seq has been successful before continuing analysis. The FASTQ file from Illumina comes with a systematic identifier before each read. The systematic identifier contains information about the reads such as when the read was sequenced, which cluster on the glass plate the read was from and which member of a pair the read was.

After sequence quality was approved, the analysis proceeded with aligning the reads to the reference genome (mapping). A mapping is regarded correct if the read overlaps the right region in the genome, and an alignment is the detailed placement of each base in a read, and is regarded to be correct if each base overlaps the right base of the genome. Therefore it is often necessary to refine the mapping to get the right alignment.

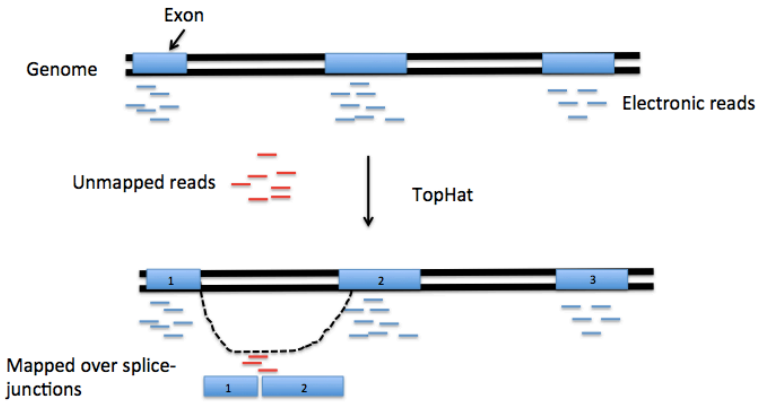

Figure 13 Mapping reads with TopHat First all the reads that fall within the exons (blue) are aligned with Bowtie. Then TopHat maps the reads (red) that map over exon-exon junctions.

In this RNA-seq analysis pipeline the mapping was performed by the free open-source software Bowtie and TopHat. Both Bowtie and TopHat are UNIX-based, but there exists a graphical interface provided by the Galaxy project online (https://main.g2.bx.psu.edu/). Bowtie is based on the Burrows-Wheeler Transform (BWT). BWT is a computer algorithm for finding the location of substrings (reads) within a string (reference genome). TopHat is built on Bowtie and can map the reads that spans over the introns (splice junctions). These reads on the splice junctions would normally fail to be read because they do not map continuously to the genome (Trapnell et al 2009). TopHat finds these junctions by performing the procedure in two steps (figure 13). First TopHat uses Bowtie to map all reads, and then it searches all the reads that was not originally mapped and find the splice-sites. TopHat finds about 70 % of all exon splice junctions, according to Trapnell, 2009. The reads where mapped to the medaka genome available at Ensembl (http://www.ensembl.org/index.html).

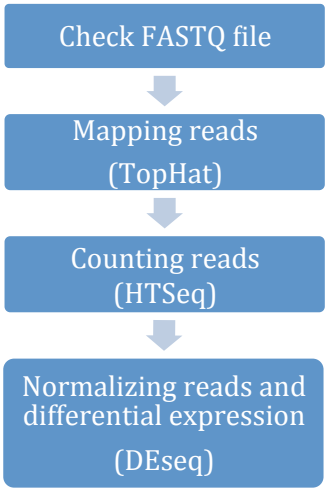

Figure 14 Overview over analysis pipeline. First the qualities of the reads are checked, then the reads are mapped to the genome with TopHat, the reads are counted with HTSeq. Thereby the reads could be normalized and find differential expression between samples with DESeq.

When all the reads are mapped to the genome, it is possible to count the reads and get an estimate of expression level of the different genes the reads align to (figure 14). The reads were counted using the HTSeq-package in Python (programming language). A software

called DESeq was used in the programming language R to normalize the counts of the reads against total numbers of reads, and to compare the expression level between the juvenile and the adult samples. Differential expression is represented with a heat map, which was made with the MEV software (version 4.7.4) (Saeed et al. 2006).

2.7 Phylogenetic trees and sequence analysis

The K_{Ca} channel sequences were located in eel, medaka and cod, and a phylogenetic analyses were made of the obtained sequences. The databases NCBI (http://www.ncbi.nlm.nih.gov/) and Ensembl (http://www.ensembl.org) were used to retrieve K_{Ca} channel sequences from fish and tetrapods. Cod and medaka sequences were found by a BLAST (Basic Local Alignment Search Tool) search with known K_{Ca} channel sequences against their respective genomes (Kasahara et al. 2007; Star et al. 2011) in Ensembl. The eel K_{Ca} channel sequences were obtained by using the CLC DNA Workbench software to do a local BLAST with known K_{Ca} channel sequences against the eel genome and pituitary transcriptome (Henkel et al. 2012) (www.eelgenome.org). The eel pituitary transcriptome where used to find the exons in the channel sequences. CLC DNA Workbench software was also used to make alignments of the amino-acid sequences of the eel, medaka and cod K_{Ca} channels as presented in Results.

All the K_{Ca} channel amino acid sequences (The NCBI and Ensembl accession numbers are found in appendix 1) were aligned with Muscle (*mu*ltiple *s*equence *c*omparison by *l*og-*e*xpectation) (Edgar 2004) in SeaView 4.3.3 (Gouy et al. 2010) for phylogenetic tree construction. The alignment was then manually edited to make a best possible basis for phylogenetic tree generation. Alignments were tested with the program ProtTest (bioportal.uio.no) (Abascal et al. 2005) to find the best fitted evolutionary model. ProtTest finds the model of protein evolution that best fit a given alignment; the models are substitution matrices and also have improvements that account for evolutionary constraints. Phylogenetic trees were constructed using PHYML in SeaView 4.3.3 and bootstrap analysis was performed on 500 trees.

3 Results

3.1 Genotyping of sex

Juvenile and adult medaka were genotyped to ensure that only females were sampled for RNA-sequencing. The PCR-amplification of the DMY and DMRT1 gene were analysed by gel electrophoresis (figure 15). Since both the autosomal DMRT1 (1300 kb product) gene and the male-specific DMY (1000 kb product) gene were amplified by the same primers, a male control was required in addition to the female positive control, ensuring that both genes were amplified in the PCR and could be distinguished. However, the autosomal DMRT1 gene in males was not amplified. Despite the lack of the 1300 kb product in males, it was still possible to differentiate between the sexes. In this run (figure 15) all unknown samples were females. Out of 115 adults and 139 juveniles tested, 113 (98 %) and 101 (74 %) were females, respectively.

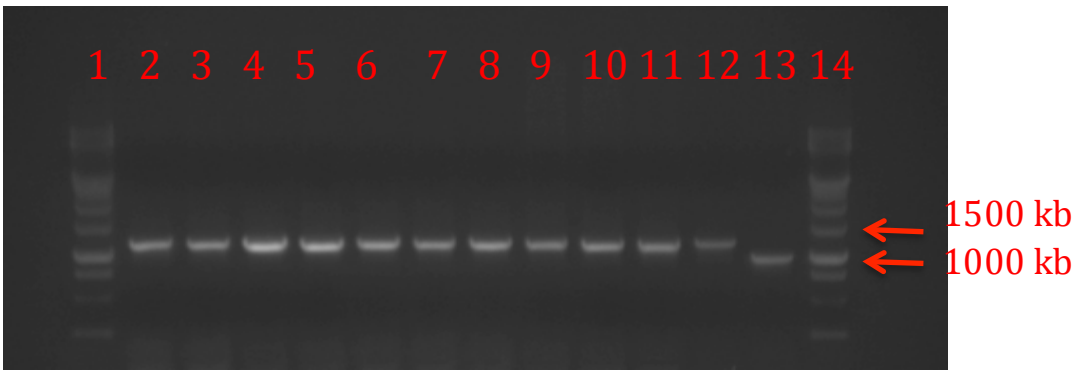

Figure 15 Genotyping of sex with PCR. Lane 1 and 14: 1 kB ladder (Invitrogen). Lane 2-11: PCR-product from phenotypically sorted females that was genotyped, all with 1300 kb product. Lane 12: Female positive control containing DMRT1 gene (1300 kb product). Lane 13: Male control containing male specific DMY gene (1000 kb product). The autosomal DMRT1 gene lacks in this male control. Note that all of the unknown samples are females in this run (lane 2-11).

3.2 FACS-sorting

The (lhb:GFP) line of medaka used in this project has the GFP gene coupled to the LHβ promoter enabling LH producing gonadotropes to express GFP (figure 16). The GFP expressing cells were sorted out from a suspension of acutely dissociated pituitary cells using the BD FACSAria instrument at Ullevål University Hospital.

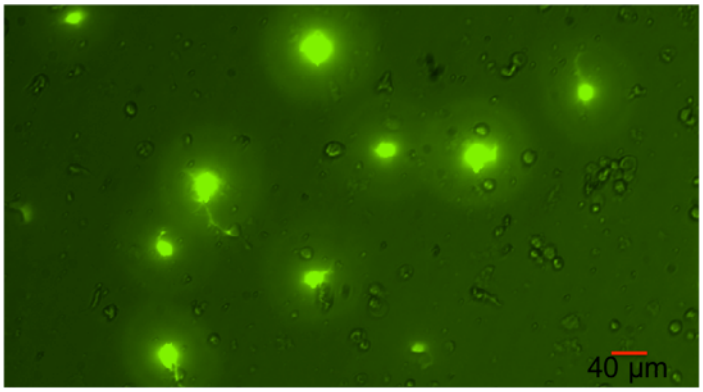

Figure 16 Dispersed pituitary cells from female adult medaka. LH-producing gonadotropes express GFP. Some of the GFP expressing cells have extensions. Note the GFP-negative cells, which are endocrine cells producing hormones other than LH. (Photo by Eirill Ager-Wick)

Adjustments and optimization were made prior to FACS sorting to identify cells with the characteristics of healthy, GFP-positive cells. Optimization should be done before FACS sorting of each new cell type (Tzur et al. 2011). The dot plot (each cell represented as a dot on a x-y graph) of the FACS sorting, visualizes the characteristics of the cells and thereby makes it possible to define characteristics of desired cells (figure 17). Adjustment was based on the size and fluorescent characteristics of the desired cells, measured by the intensity of SSC and FSC respectively. As a result of the adjustments performed on the samples prior to sorting, some GFP-positive cells were lost in the process.

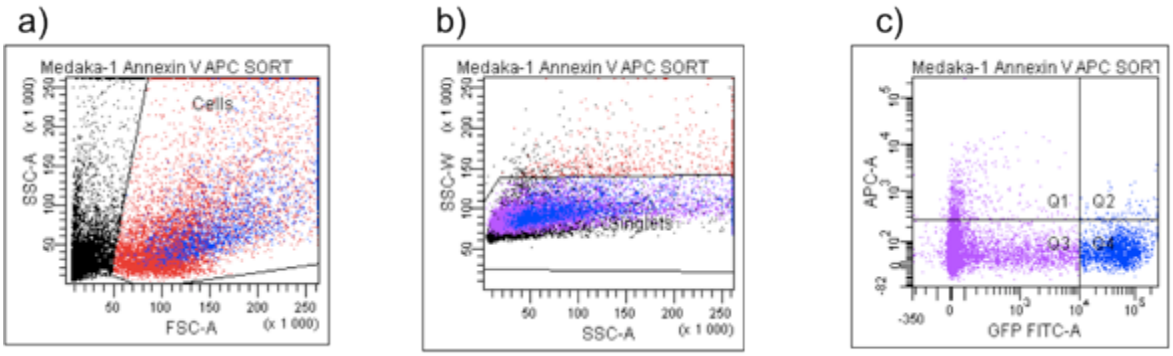

Figure 17 Determining the sorting parameters by dot-plots. a) *Excluding small fragments.* Initially the cell population to be sorted are identified based on size. Each dot represents one cell, with the x-axis indicating cell size based on forward scatter characteristics (FSC), and the y-axis indicating granularity or fluorescent characteristics based on side scatter characteristics (SSC) .The red and the blue dots represents cells that are selected for further sorting. The black dots in this plot represent small fragments and are thus excluded. b) *Excluding doublets.* The cell population is sorted on size; doublets are discriminated based on side scatter pulse width (SSC-W), where the larger cells have higher values (y-axis), and the x-axis is the same as the y-axis in a). c) *Representation of the sorting parameters based on fluorescence.* X-axis represents the intensity of APC and the y-axis represents the intensity of GFP. Cells in the lower right corner (Q4) are sorted out. These cells are healthy, have no sign of apoptosis (low APC signal) and have a strong GFP expression (strong GFP FITC signal).

The population of cells to be selected is initially identified based on size. Particles too small to be cells are excluded first (figure 17 a). Thereby, the population of cells are further sorted on size to get rid of doublets, based on side scatter pulse width (SSC-W) (figure 17 b). Otherwise a GFP-positive cell adhered to a negative cell could be recognized as a positive,

obscuring the analysis. Further, the population of singlet cells was separated based on their fluorescent characteristics. Figure 17 c) represents the analysis of two fluorescent (APC and GFP) markers with respect to each other. APC Annexin V stained the cells for apoptosis as described in Materials and Methods. The intensity of APC is presented along the y-axis, with the apoptotic cells at higher values. The GFP is presented along the x-axis, with the stronger GFP at higher values. The cells that had the characteristics of Q4, a low APC intensity and a high GFP intensity, were selected. Figure 18 gives an overview of the amount of cells that were sorted in each condition. Compared to the total amount of cells from the pituitary, there were few GFP-positive cells. The small peak far right represents the cells selected for further analysis.

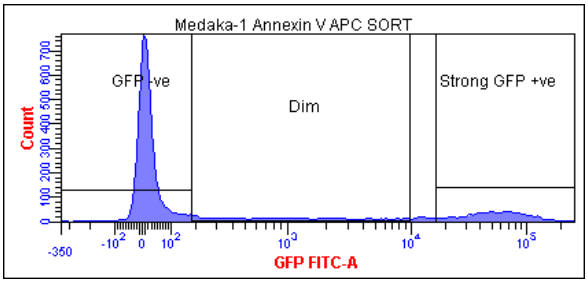

Figure 18 Overview of the sorted cells. a) Overview of how many cells that was sorted out in each condition in the same sorting as figure 17. The y-axis represents the count of cells that are sorted in each condition and the x-axis represents the intensity of GFP-expression. There are few GFP positive cells compared to the total count of cells from the pituitary. The small peak far right marked "strong GFP + ve" represents the cells that were used for further analysis.

The output from the juvenile and adult pituitaries was quite different regarding the total number of GFP positive cells (table 1), the number being considerably lower in juveniles. From 60 adult pituitaries, we got 80 000 GFP positive cells, resulting in 100 ng of RNA, in contrast to the juvenile sample where 120 pituitaries resulted in 13 000 GFP positive cells and only 12 ng of RNA. The low output of cells from juveniles resulted in a similarly low output of RNA making it necessary to pre-amplify cDNA before the Illumina sequencing to have enough template (the minimum required RNA for the RNA-seq protocol at the time of sequencing was 1 µg). The cDNA synthesis and amplification process were performed as described in Materials and Methods and resulted in 4,8 µg and 3,0 µg cDNA in the adult and juvenile sample, respectively.

Table 1 Table of the output of cell sorting, RNA isolation and amplification. Note that there are a considerably lower number of GFP cells from the juvenile medaka despite doubling the amount of fish.

	Pituitaries	GFP positive cells	RNA (ng)	cDNA (µg)
Juvenile	120	13 000	12	3,0
Adult	60	80 000	100	4,8

3.3 RNA-sequencing

3.3.1 Quality of the sequenced reads

From each run on the Illumina platform, a FASTQ file is provided where the quality scores for each base of a read is implemented. These quality scores may be visualized in plots, to inspect the quality of the reads and possibly exclude reads or trim (remove) some parts of the sequences before continuing analysis. For paired-end (sequenced from both ends) reads quality score plots are provided for each member of a pair.

Figure 19 gives an overview of the quality scores of all reads from one member of the pair-end reads from one of the adult samples. A quality score of 30 indicates a probability that 1 out of 1000 bases are incorrectly sequenced based on the template. A quality score above 28 is generally considered very good as indicated with green background colour (figure 19). Quality scores above 20 are considered acceptable (orange), and quality scores below 20 are considered insufficient (red). Yellow boxes represent the inter-quartile (25-75 %) range of the reads, and the black whiskers are at 10 % and 90 %. In this example the quality of the first 8 bases was lower than the following bases; according to the manufacturer of Ovation RNA-seq amplification kit, this is an artefact from the cDNA pre-amplification process. The first 8 bases were therefore trimmed from the sequence prior to analysis. As expected when using the Illumina technology, the read quality decreased towards the end of each read.

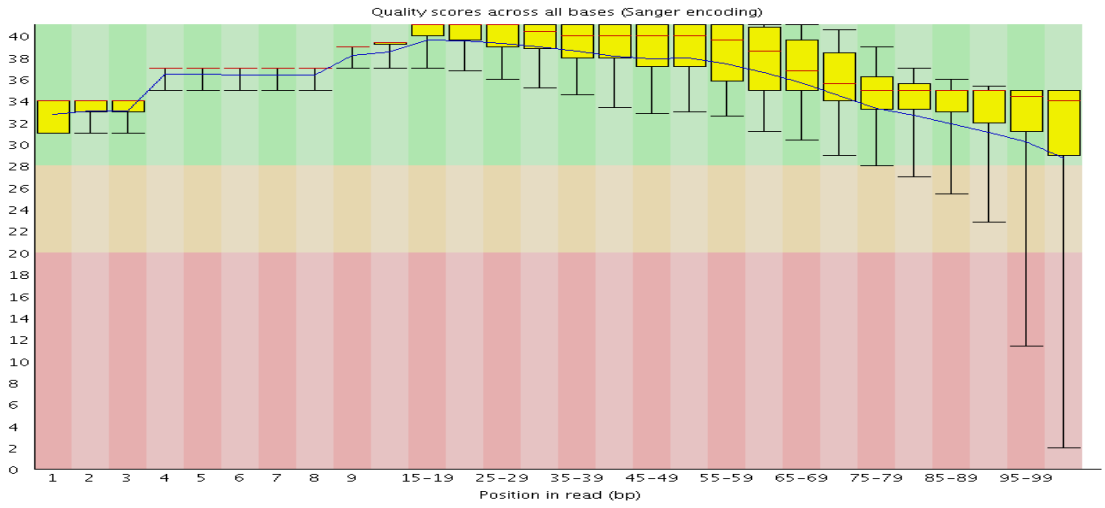

Figure 19 RNA-seq quality scores across bases of all reads. The X-axis represents position in read (bp) and the Y-axis represents the quality score for each base. The quality scores are calculated from all the reads (81 119 072) from the adult sample in this example. The yellow box is the inter-quartile range, the upper and lower black whiskers represent the 10 % and 90 % respectively. The red line and the blue line are displaying the median and the mean of the quality values respectively. The background colours indicate whether the quality scores are good (green), acceptable (orange) or bad (red). Overall the quality for these reads is very good (all of the quality scores fall within the green area). However the first 8 bases in every read show a lower quality than the following bases.

One should consider the distribution of quality scores for all the reads (figure 20) to potentially exclude subsets of reads with a lower quality, given the possibility of obscuring the analysis. The mean quality of the sequence on the x-axis is plotted against the number of

reads at the y-axis. The majority of the reads are clustered around a quality of 38, which indicates very good quality. There are no subsets of reads that show a substantially lower quality.

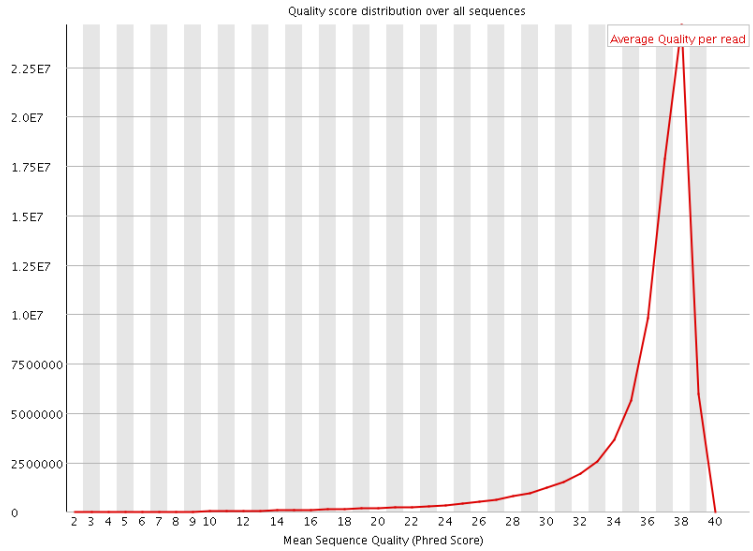

Figure 20 Quality score distribution over all sequences. This plot is generated to assess whether the quality scores are evenly distributed among the reads. The X-axis shows the average quality score and the Y-axis shows number of reads. The quality scores among all the reads are good, and there are no subsets of reads with a substantially lower quality.

3.3.2 Mapping of reads onto the medaka genome

Mapping of the reads onto the medaka genome (Ensembl.org, 2006) was performed with the software TopHat. Only the part of the medaka genome assembled into chromosomes (about 90 % of the genome) was used for mapping. Consequently, some of the reads could originate from genes belonging to the part of the genome assembled in scaffolds, and thus be overlooked in the analysis.

Over 90 % of the reads from both juvenile and adult samples mapped onto the genome. Expression of genes was counted using DEseq, and genes with expression value > 1 from DESeq was defined as being expressed (figure 21). In the sample from juvenile medaka 70 % of the annotated genes were expressed, compared to 78 % in the adult medaka sample.

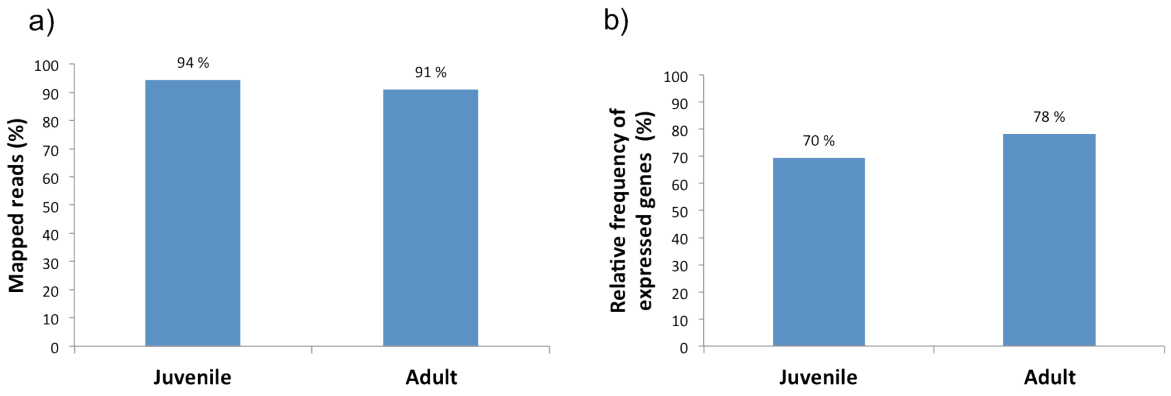

Figure 21 Overview of and expression. a) Overview of reads mapped to the medaka genome using TopHat**.** The y-axis represents percentage of mapped reads. From the sequenced juvenile sample 94 % of the reads mapped to the genome while 91 % of the reads from the adult sample mapped to the genome. **b)** The total amount of genes expressed. The y-axis represents the percentage of genes expressed compared to total amount of genes (that are assembled in chromosomes). In the juveniles 70 % were expressed (expression value >1 from DESeq), while 78 % of the adult genes were expressed (expression value >1 from DESeq)

3.3.3 Gene expression in female medaka gonadotropes

I have chosen to focus on the expression of GnRH-R, LHβ-subunit and the dopamine receptors since these genes are involved in puberty. I have also focused on the K_{Ca} channels; these results are presented in 3.4. The gene expression is measured in counts of reads mapping to the gene transcripts, the counts are normalized in the software DESeq, which also estimate the count of reads on each transcript. There is a relatively low expression of the GnRH-R3 in adult medaka (count of 4), compared to no detected expression in the juvenile sample. It is not possible to say anything about the expression of the other GnRH-R in this analysis, as the genes for other GnRH-R's are located on the scaffolds, which were not included in this analysis. The LHβ-mRNA show massive expression in both adult and juvenile, with 21715 and 32447 counts respectively. The corresponding GPα-mRNA that is the subunit similar for FSH, LH and TRH was similarly highly expressed, with 112444 counts from the adult sample and 39902 counts from the juvenile sample, which means a 2.8 fold change from juvenile to adult. The dopamine receptor1-3 ($D_{1\text{-}3}$) was expressed. D_1 (count of 92) and D_3 (count of 264) were expressed more in juveniles than in adults, where D_1 had a count of 15 and D_3 had a count of 114. However the D_2 receptor was expressed more in the adults than the juveniles, with 1658 and 1423 counts respectively. The fold change was greater for the two receptors (D_1 and D_3) more highly expressed in juveniles.

Figure 22 represents the hundred most differentially expressed genes between the juvenile and adult based on fold change. However, since a large-scale analysis of the gene expression levels in my samples was out of the scope of this master thesis, I have not included additional information about the differentially expressed genes in the figure. The figure is included to illustrate that there are indeed differences between the samples.

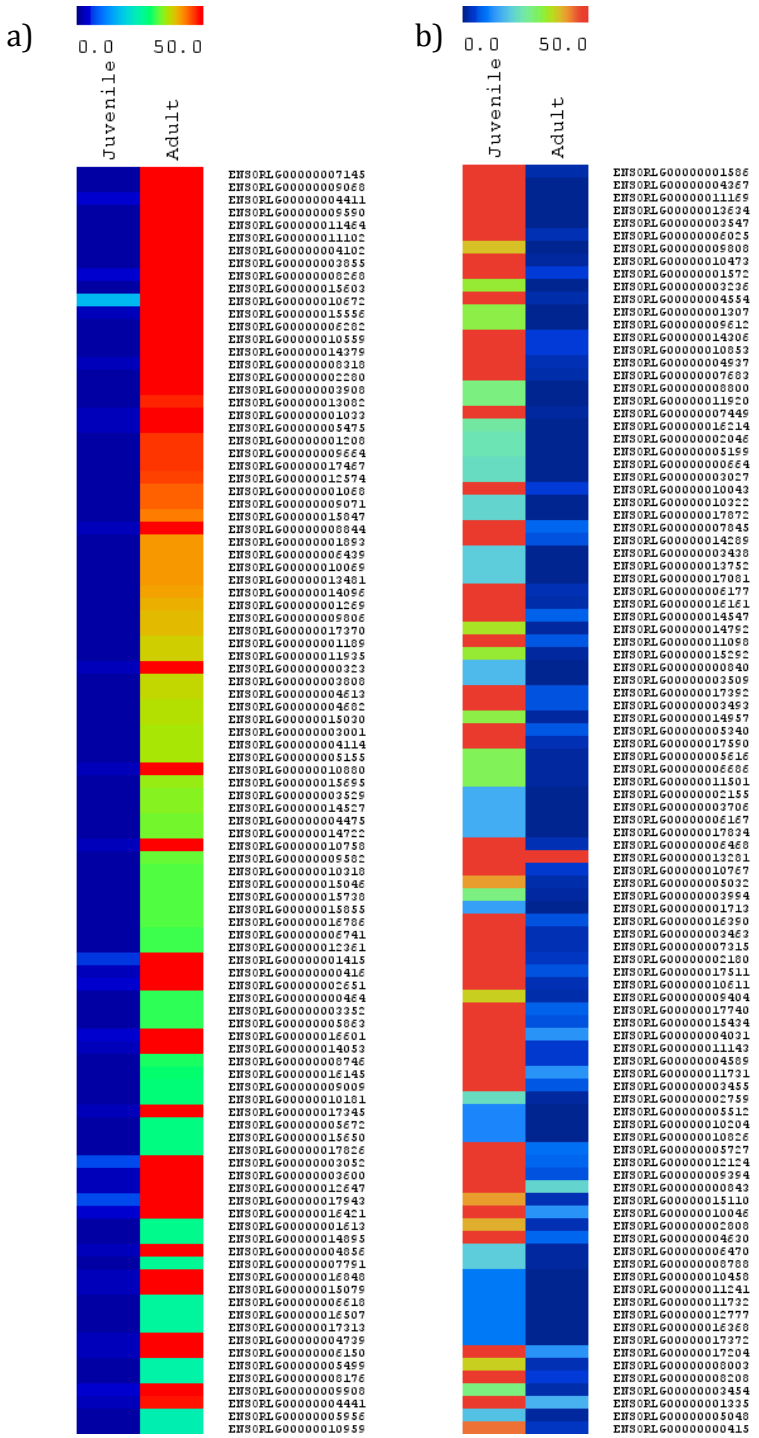

Figure 22 Heat map of the hundred most differential expressed genes based on fold change. a) Higher expression in adult than juvenile. b) Higher expression in juvenile than adult. The colours indicate the count of the reads mapping to the transcript, ranging from 0 (blue) to 50 (red).

3.4 K_{Ca} channels

The K_{Ca} channels are involved in the control of electrical excitability in the gonadotropes. Our group has studied these channels with electrophysiological techniques and is interested in

more detailed knowledge on how these channels are expressed in gonadotropes of the model organisms (cod, eel and medaka). Differences between the two gonadotrope subtypes, between sexes and between juvenile and adult fish may be expected.

3.4.1 Expression of K_{Ca} channels in LH-producing gonadotropes

All of the K_{Ca} channels were expressed in both adult and juvenile female medaka, except for one of the two KCNN1 (variant 2 of 2) that was not expressed in neither juvenile nor adult. The expression levels in adult and juvenile samples were similar for all the channels analysed (figure 23).

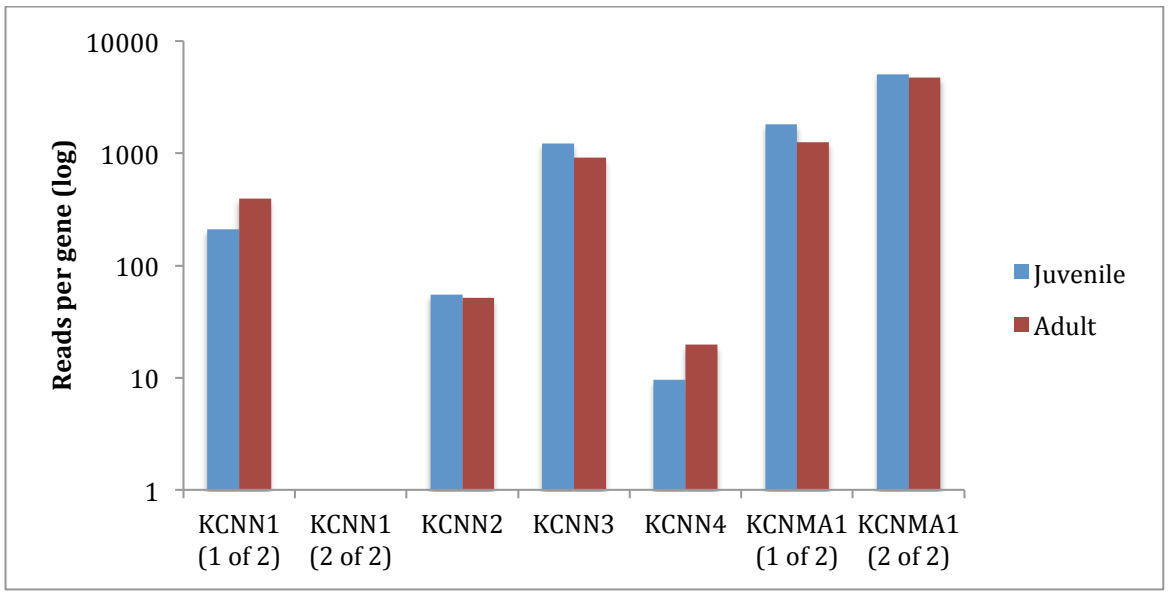

Figure 23 Expression of the different K_{Ca} channels in the LH-producing gonadotropes. The Y-axis shows a logarithmic scale of the counts per gene. With an exception of one of the KCNN1-genes, all channels were expressed both in juveniles and adults and no large differences were found in expression between the two samples.

3.4.2 Alignments of eel, cod and medaka K_{Ca} sequences

The K_{Ca} sequences from eel, medaka and cod were obtained by searching their respective genomes with BLAST, as described in Materials and Methods, and the sequences were aligned with CLC DNA Workbench software for figure representation. For eel, sequences were only obtained for the BK channel, the SK1 channel and SK2 channel. The parts of the eel sequence that seem to be genuine sequences are marked with red and green vertical lines in the figures (figure 24-28). The K_{Ca} channels are highly conserved through all vertebrates, it is therefore expected that the eel sequence will be similar in the areas of all the functional domains.

In medaka and cod there exist two versions of the BK channel sequence. For eel, on the other hand, only a small part of one sequence was obtained and there was no evidence for a second

version (figure 24). The two BK versions (designated A and B) were almost identical, with minor differences in the amino acid sequences. Marked with horizontal blue lines are two segments of the alignment where the BK A-variant of cod and medaka differs from the BK B-variant.

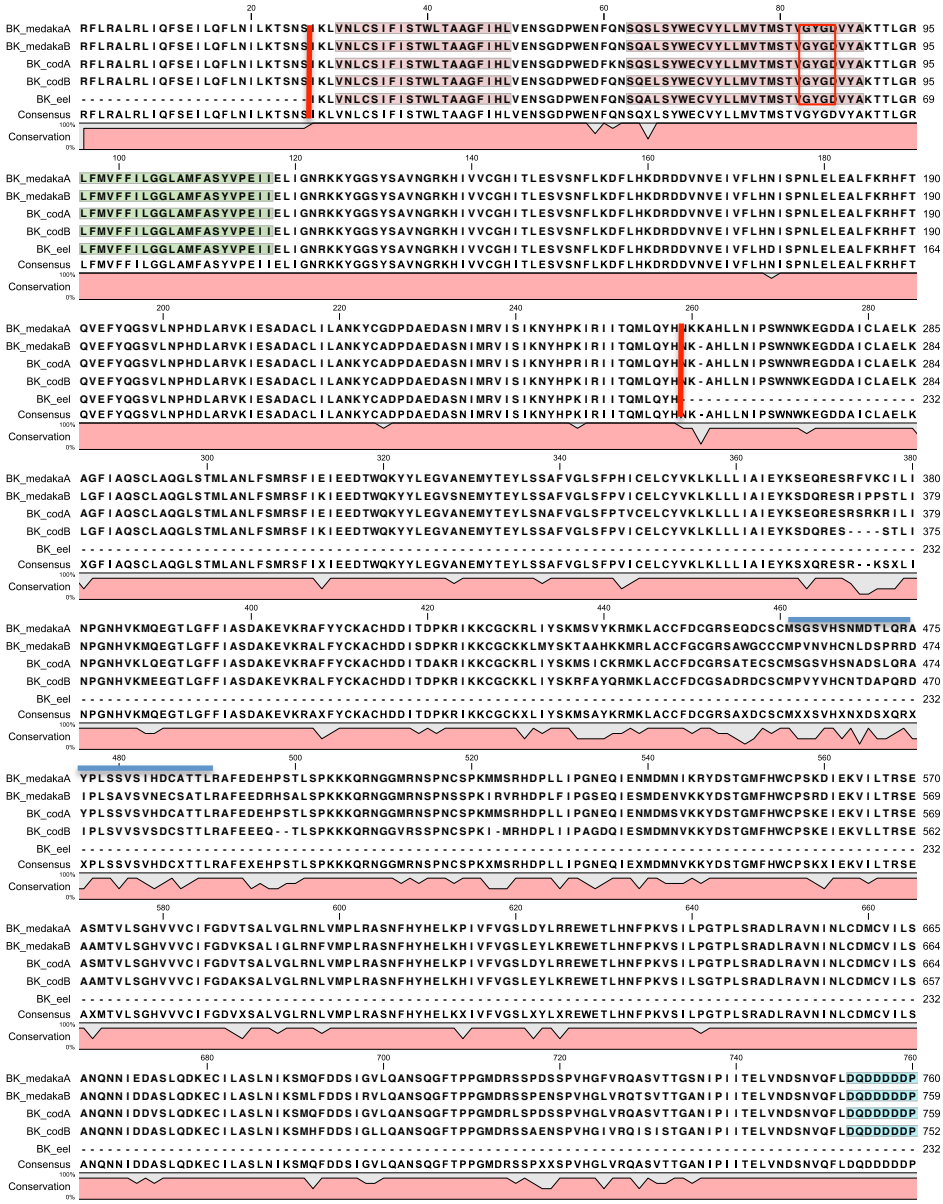

Figure 24 Alignment of BK channel sequence. The alignment was generated with the CLC DNA Workbench software. Percentage of conservation is displayed in pink under the alignment. The S4 and S5 region in the BK channels are highlighted in pink, the pore-containing region is highlighted in green and the calcium bowl is highlighted in blue. The K_{Ca} signature sequence (GYGD) is marked with a red box. The eel-sequence that was obtained is marked with 2 red vertical lines. The term A and B is designed to separate the two genes from cod and medaka derived from separate chromosomes/scaffolds. Marked with horizontal blue lines are stretches of the sequences where version a and version b of cod and medaka sequence corresponds. (MedakaA corresponds to (1 of 2) and medakaB corresponds to (2 of 2) in figure 23).

Similarly two versions of the SK1 gene also exist in cod and medaka, while only one version was obtained from eel (figure 25). The SK1 sequence that was found in eel was aligned to the cod and medaka SK1 sequences, and the segments of the sequence that most likely are correct

are marked with red vertical lines (the part that was used for phylogenetic analysis), and green vertical lines. However, within the area where the eel sequence was found, a poorly sequenced region of the cod SK1 sequence (SK1_codA) was evident, and the entire sequence was therefore removed from the phylogenetic analysis. Similarly to the BK channel, some stretches of the sequence had the same amino acids replacement in both cod and medaka, where the A sequence from cod was similar to the A sequence from medaka. The A-sequence of both medaka and cod was longer than the B-sequences.

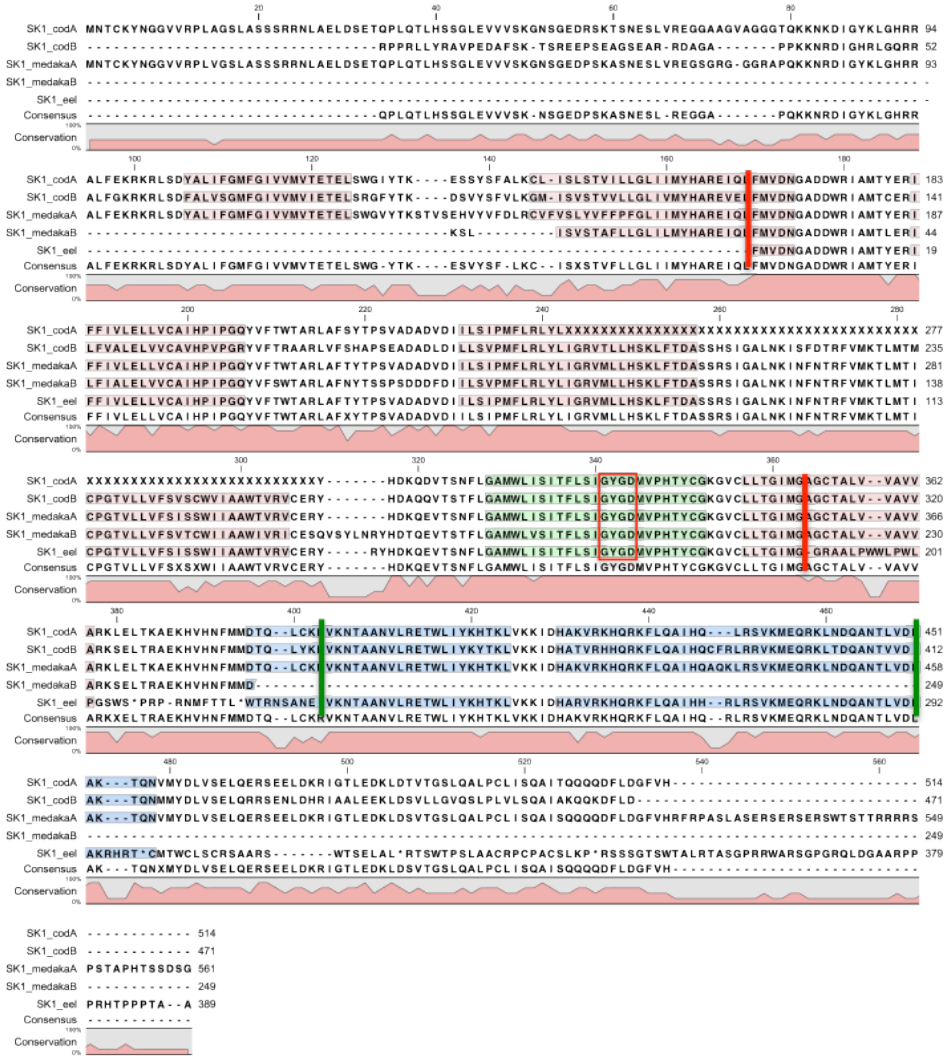

Figure 25 Alignment of the SK1 channel sequences. The alignment was generated with the CLC DNA workbench. Percentage of conservation is displayed in pink under the alignment. The S1-S5 regions in the SK1 channels are highlighted in pink, the pore-containing region is highlighted in green and the calmodulin-binding domain is highlighted in blue. The K_{Ca} signature sequence (GYGD) is marked with a red box. The eel-sequence that was most likely a genuin sequence is marked with two red vertical lines (part of the sequence used for the tree generation) and green vertical lines. The term A and B is designed to separate the two genes from cod and medaka derived from separate chromosomes/scaffolds. Medaka A corresponding to version (2 of 2) and medakaB corresponds to version (1 of 2) in figure 23. (Annotation of SK-sequences from Cong et al, 2009)

The part of the SK2 channel sequence from eel that appears to be genuine is marked with two red vertical lines (figure 26). The part of the eel sequence not marked with vertical lines is most likely out of reading frame, since the SK channel sequences are highly conserved among vertebrates. SK2 channel sequences were found for both medaka and cod, and the sequences are similar, with an exception of a few amino acids.

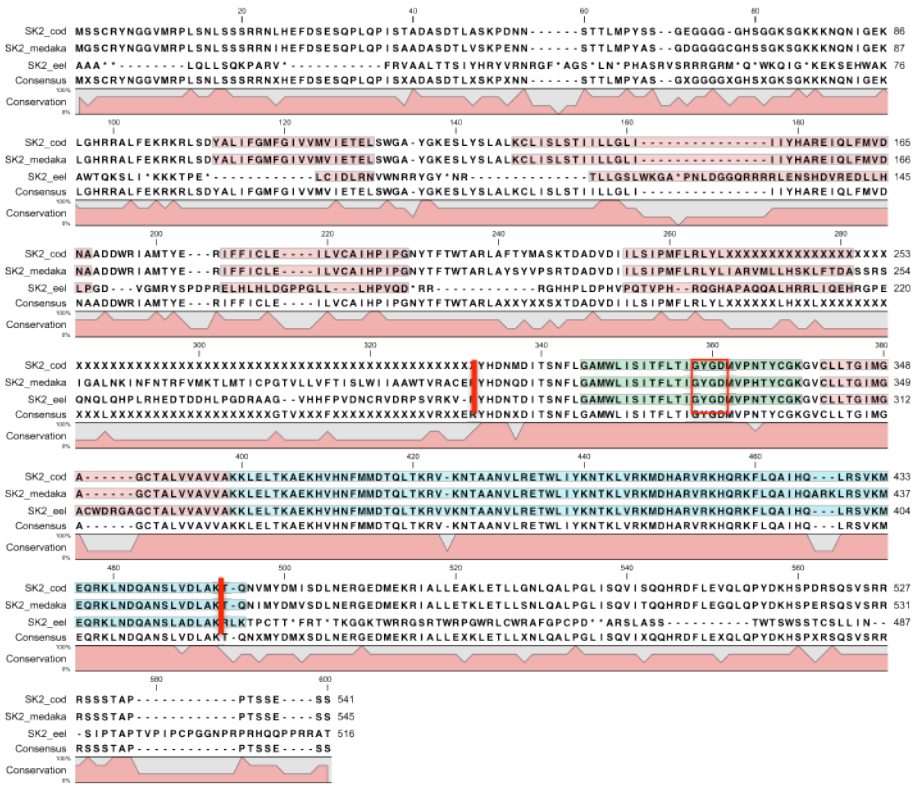

Figure 26 Alignment of SK2 channel sequence. The alignment was generated with the CLC DNA workbench. Percentage of conservation is displayed in pink under the alignment. The S1-S5 regions in the SK1 channels are highlighted in pink, the pore-containing region is highlighted in green and the calmodulin-binding domain is highlighted in blue. The K_{Ca} signature sequence (GYGD) is marked with a red box. The part of the eel-sequence that is most likely a genuine sequence is marked with two red vertical lines; this was the part of the sequence used for the tree generation. (Annotation of SK-sequences from Cong et al, 2009)

The SK3 and IK channel sequences were not found in eel, while both channel sequences were found in medaka and cod (figure 27 and 28). The medaka and cod sequences are very similar to each other, but differ in some amino acids when it comes to both SK3 and IK. The cod SK3 channel sequence is shorter than the medaka sequence, possibly because some part of the sequence is missing in the published genome (figure 27). The IK sequences are less similar between cod and medaka, than the two SK3 sequences (figure 28). The part of the sequences used for phylogenetic analysis is marked with red vertical lines in both figures.

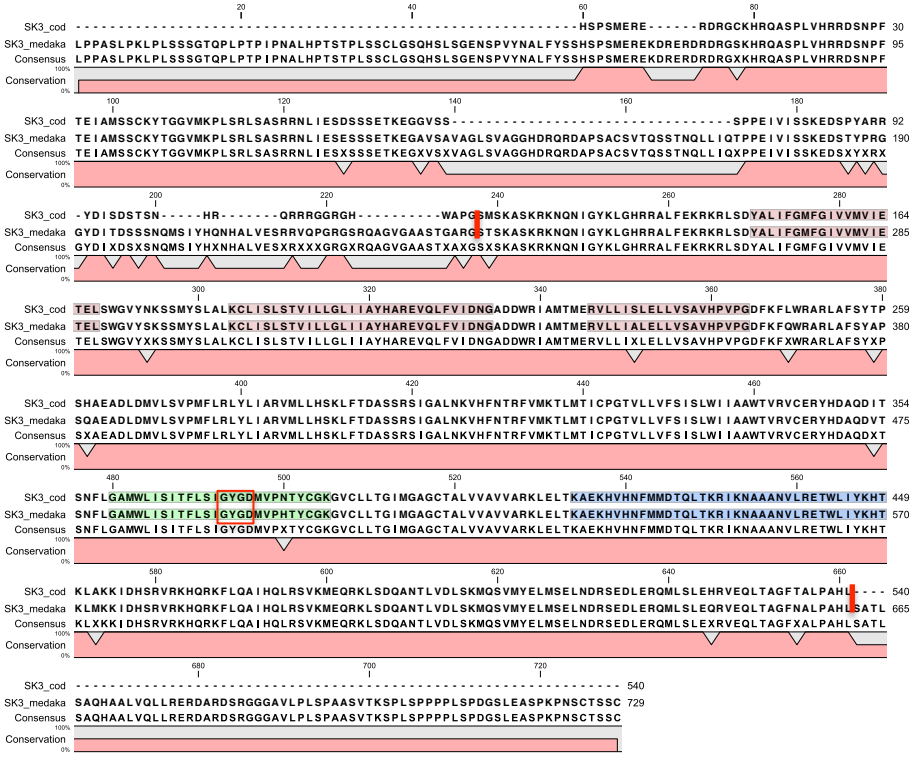

Figure 27 Alignment of SK3 channel sequence. The alignment was generated with the CLC DNA workbench. Percentage of conservation is displayed in pink under the alignment. The S1-S5 regions in the SK1 channels are highlighted in pink, the pore-containing region is highlighted in green and the calmodulin-binding domain is highlighted in blue. The K_{Ca} signature sequence (GYGD) is marked with a red box. The part of the sequence used for phylogenetic analysis is marked with two red vertical lines. (Annotation of SK-sequences from Cong et al, 2009)

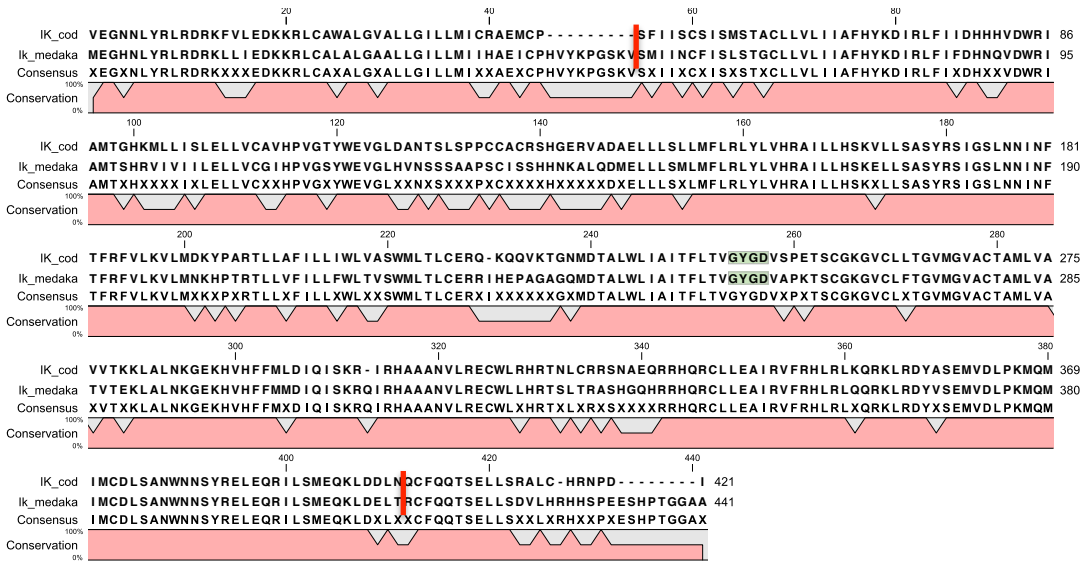

Figure 28 Alignment of IK channel sequence. The alignment was generated with the CLC DNA workbench. Percentage of conservation is displayed in pink under the alignment. The K_{Ca} signature sequence (GYGD) is marked with green highlighting. Percentage of conservation is displayed in pink under the alignment. The part of the sequence between the two red vertical lines is used in the phylogenetic analysis.

3.4.3 Phylogenetic trees

Phylogenetic trees were constructed as described in Materials and Methods (for gene accession numbers, see appendix 1). Trees of the individual channels were based on a small section of the sequences where also the eel-sequence was found reliable (figure 24-28). These subsets are highly conserved among vertebrates, and thus the sequences are very similar.

In all the trees of the individual channels, the teleosts and mammals branch off in distinct clads reflecting their evolutionary relationship. The eel sequence branch off earlier than the other teleost sequences in the BK channel tree (figure 29). However, in the two other trees (SK1 and SK2) the eel sequence is among the other teleost channel sequences (figure 30 and 31). In the phylogenetic tree analysis of the BK channel, the two variants found in cod seem to be more closely related to each other, than to the channel sequences from the other teleosts. However, this is different in the phylogenetic tree of all the K_{Ca} channels, where a larger stretch from the BK-channel sequences was used. Here the two A variants (codA/medakaA) clusters together, and the two B-variants clusters together (codB/medakaB) (figure 34).

In the phylogenetic analysis of SK1, one of the variants from cod and one from medaka branch off earlier than the other sequences. Further, the other SK1 sequences split into two distinct clads consisting of mammalian sequences in one, and teleost sequences in the other clad. The phylogenetic trees of the SK3 and IK channel both show that the teleost sequences and the mammalian sequences branch off in two distinct clads from a common ancestor (figure 32 and 33).

Furthermore, a phylogenetic analysis of all the K_{Ca} channel sequences together reveals two distinct clads, where one clad consists of BK channel sequences and the other consists of the more interrelated channels SK1-3 and IK (figure 34). The clad consisting of the small and intermediate K_{Ca} channel sequences separates further in two, the three SK channels in one clad and the IK channel in another, precisely mirroring the well-known phylogenetic relationship.

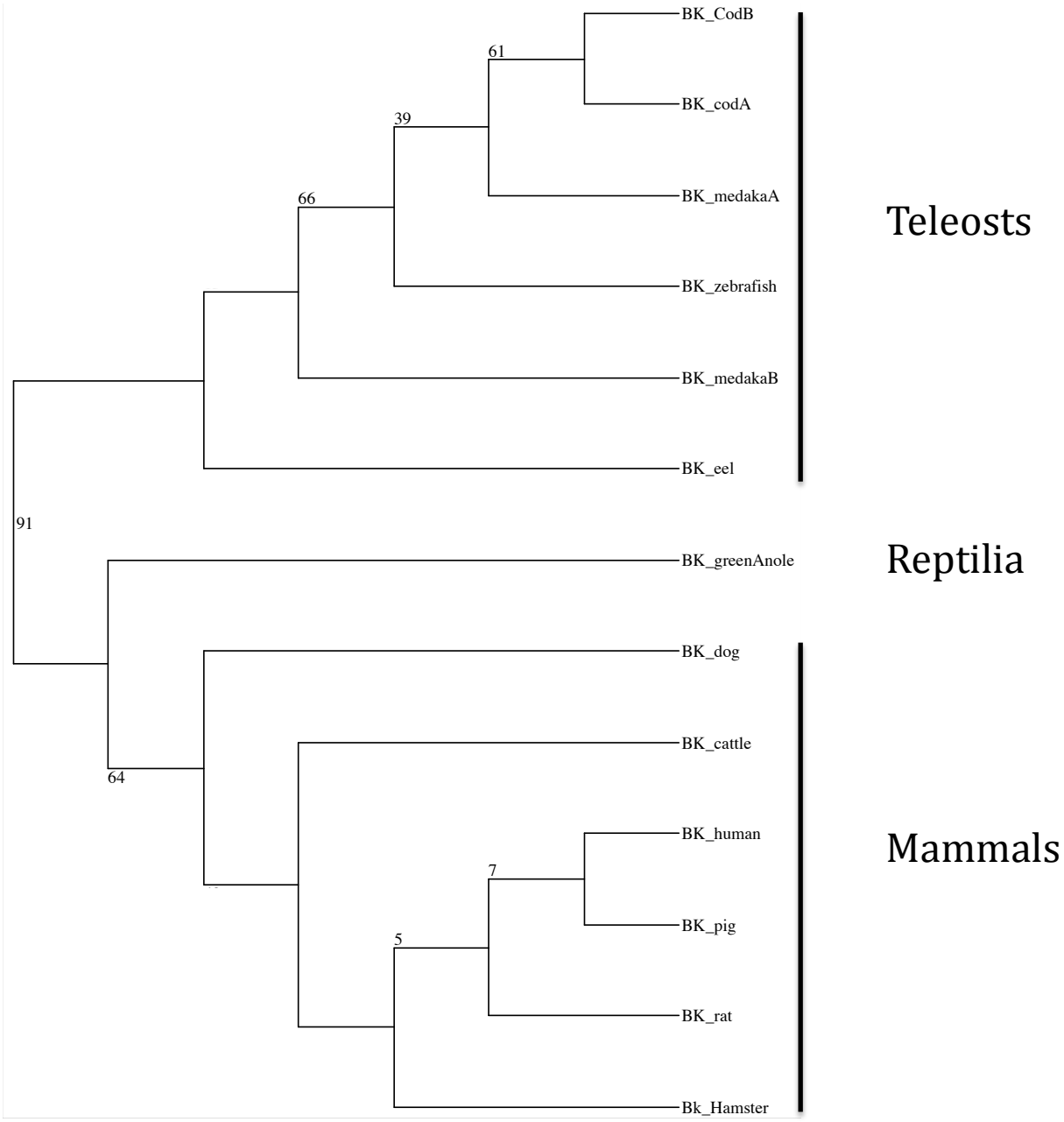

Figure 29 BK channel phylogenetic tree Phylogenetic tree was constructed by a maximum likelihood analysis with PHYML. The tree was drawn in SeaView 4 software with an evolutionary replacement model generated by ProtTest. Bootstrap analysis was performed on 500 data sets. Bootstrap values greater or equal to 50 are implemented in the figure. The phylogenetic tree is presented as an unrooted cladogram. All the channels reference number is in appendix 1. The teleosts branch off in one clad while mammals and reptile branch off in another clad, the reptile branch off before the mammals. The eel-sequence is in the group of teleosts but seem to have branched of before the other teleosts as expected. Due to the small part of the BK-channel obtained from eel, the analysis was performed on a short region that is highly conserved among vertebrates. All gene accession numbers could be found in Appendix 1.

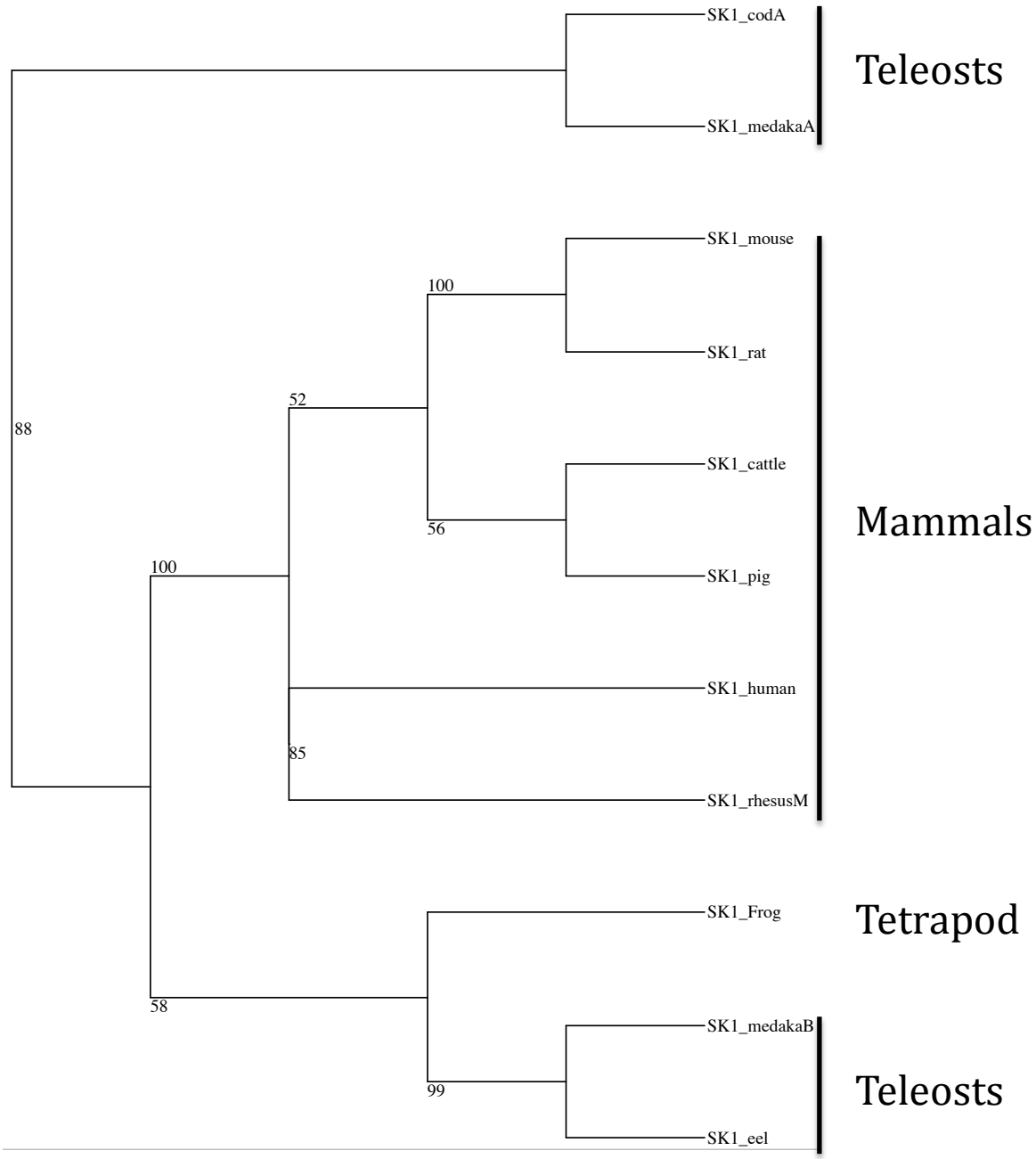

Figure 30 SK1 channel phylogenetic tree. Phylogenetic tree constructed as in figure 29. Medaka and cod has two SK1 – genes, one of the SK1 genes from each organism branch off earlier than the other sequences. Originating from this SK1 variant, the phylogenetic tree branch off in two more clads, one consisting off the mammalian sequences and the other clad consisting of teleost and amphibian sequences. The other SK1-gene variant from cod was removed from the analysis because the part of the sequence that was used for the tree generation was poorly sequenced. All gene accession numbers could be found in Appendix 1.

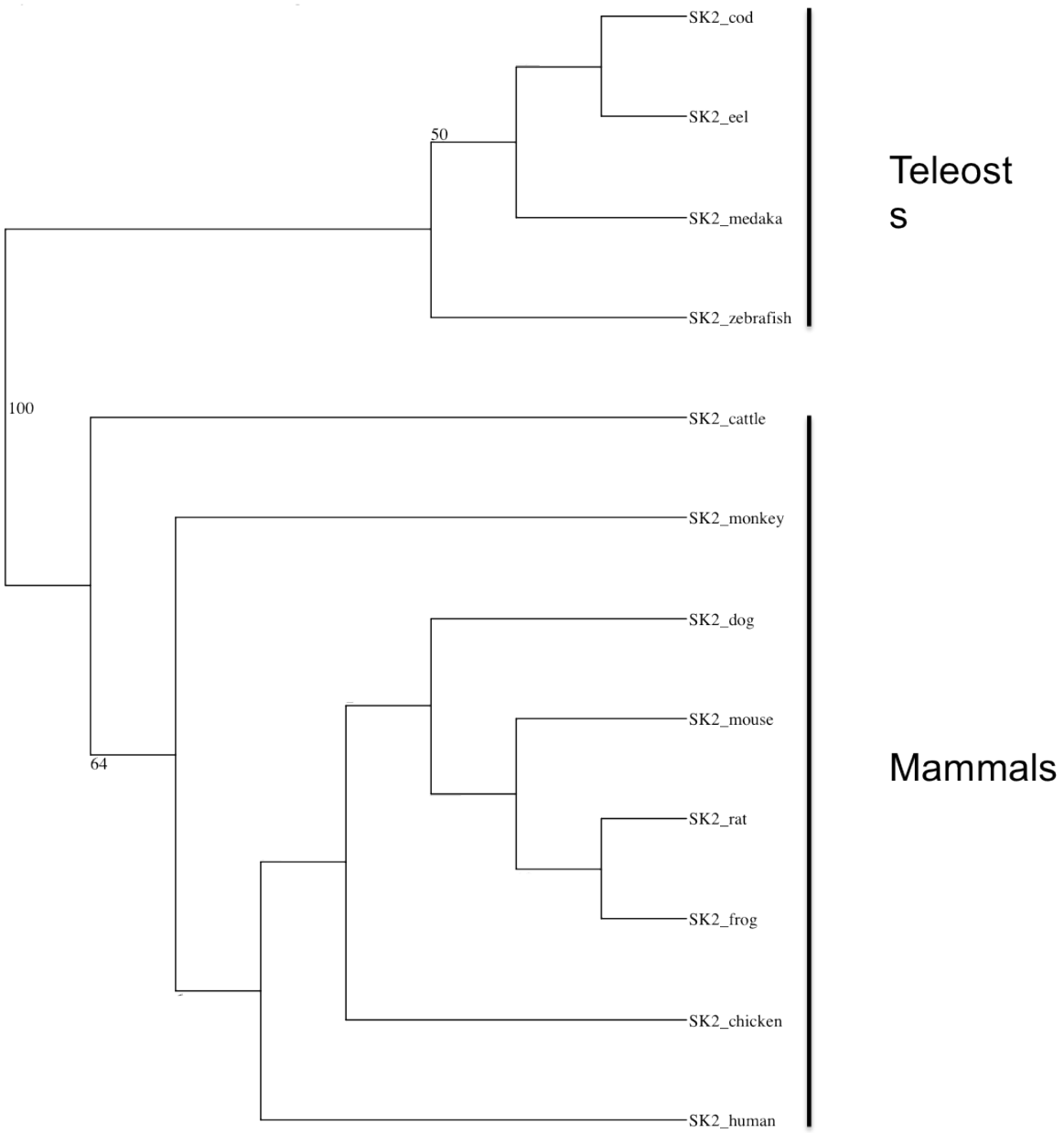

Figure 31 SK2 channel phylogenetic tree. Phylogenetic tree constructed as in figure 29. Here the teleosts sequences branch off in one clad. The eel sequence is branch off together with the other teleosts. The other clad consists of tetrapods, including mammal, bird and amphibian sequences. All gene accession numbers could be found in Appendix 1.

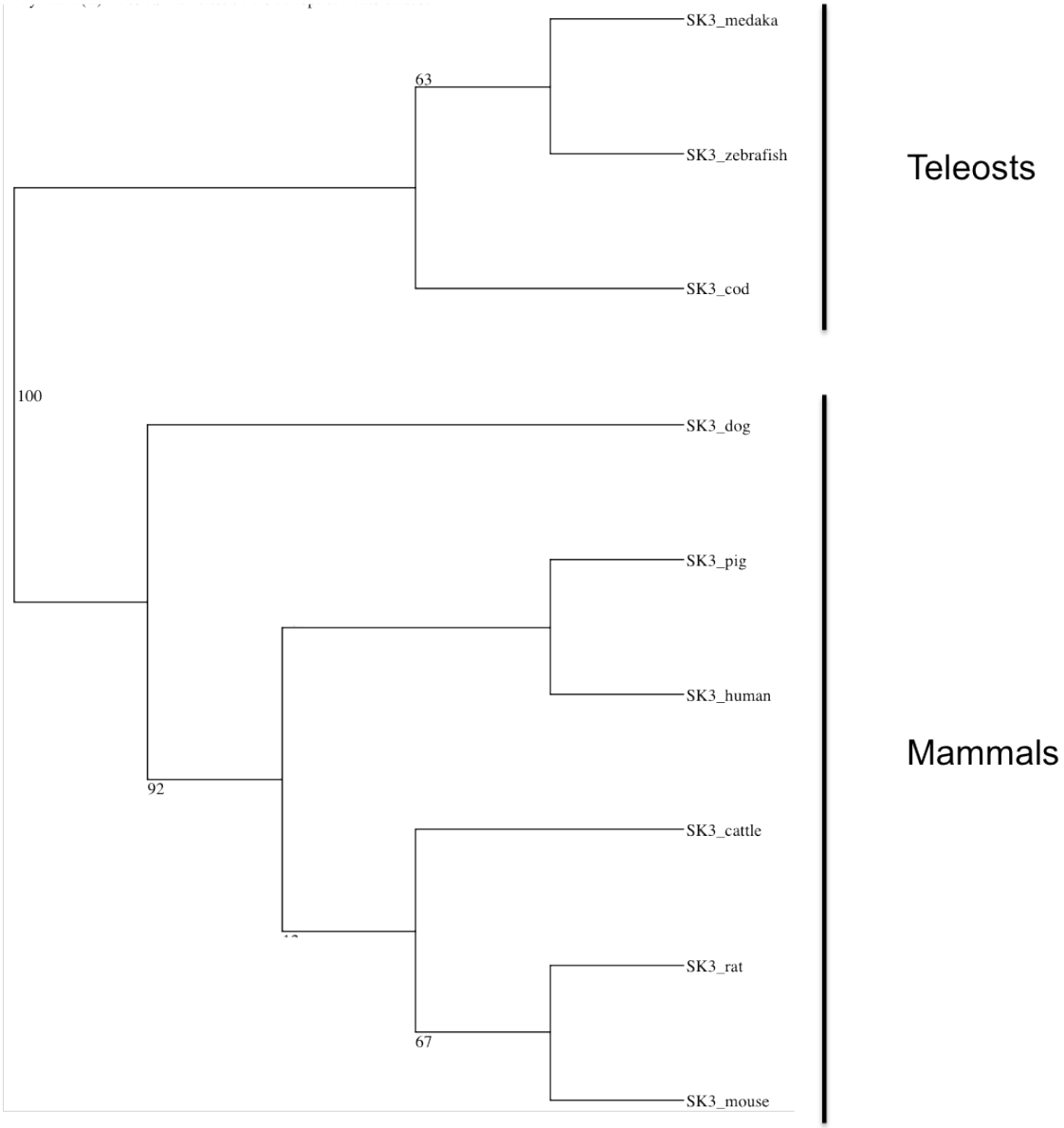

Figure 32 SK3 channel phylogenetic tree. Phylogenetic tree constructed as in figure 29. The teleost and the mammalian sequences branch off in two distinct clads. All gene accession numbers could be found in Appendix 1.

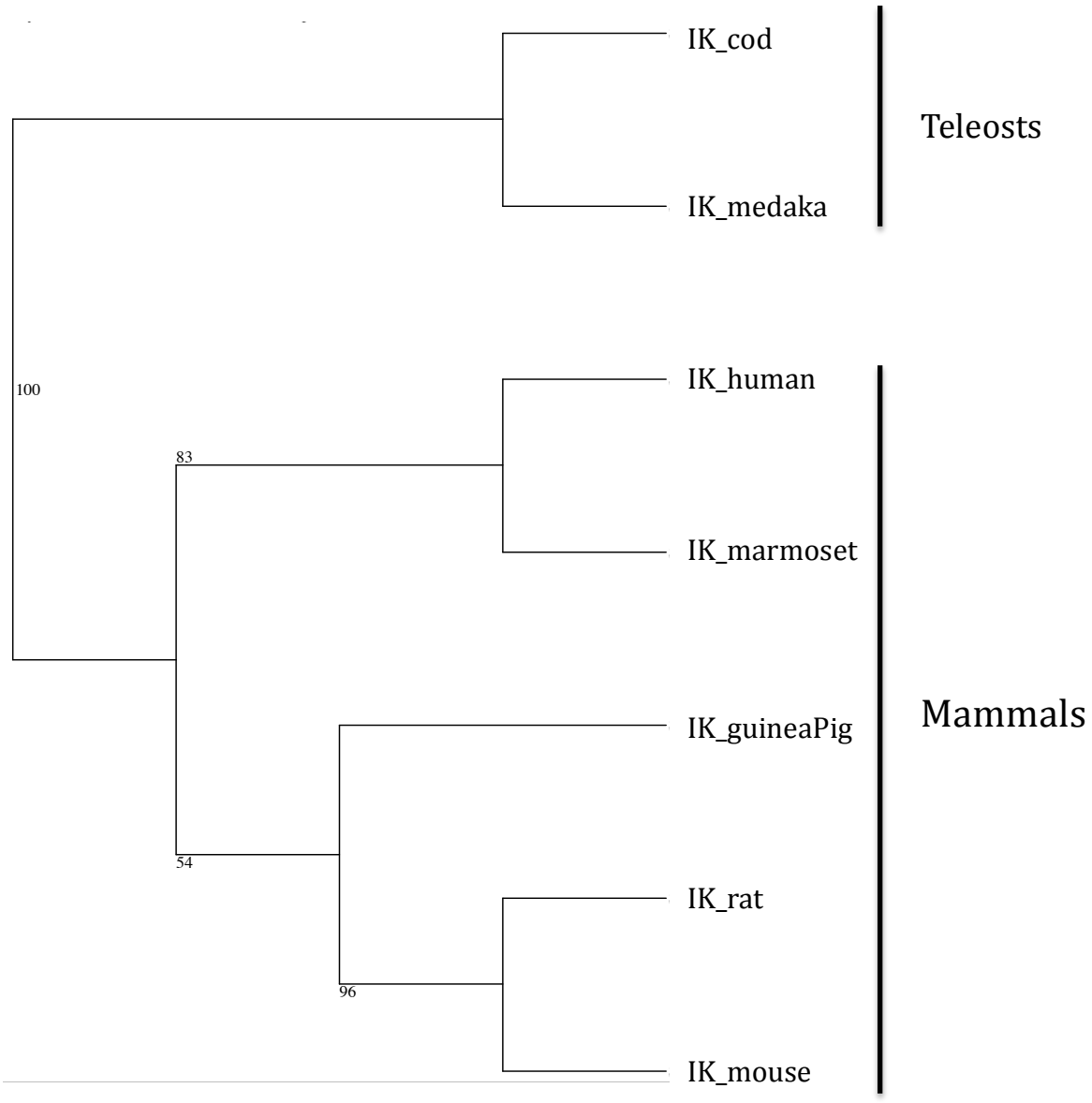

Figure 33 IK channel phylogenetic tree. Phylogenetic tree constructed as in figure 29. The mammalian and the two teleosts sequences branch off in two distinct clads. All gene accession numbers could be found in Appendix 1.

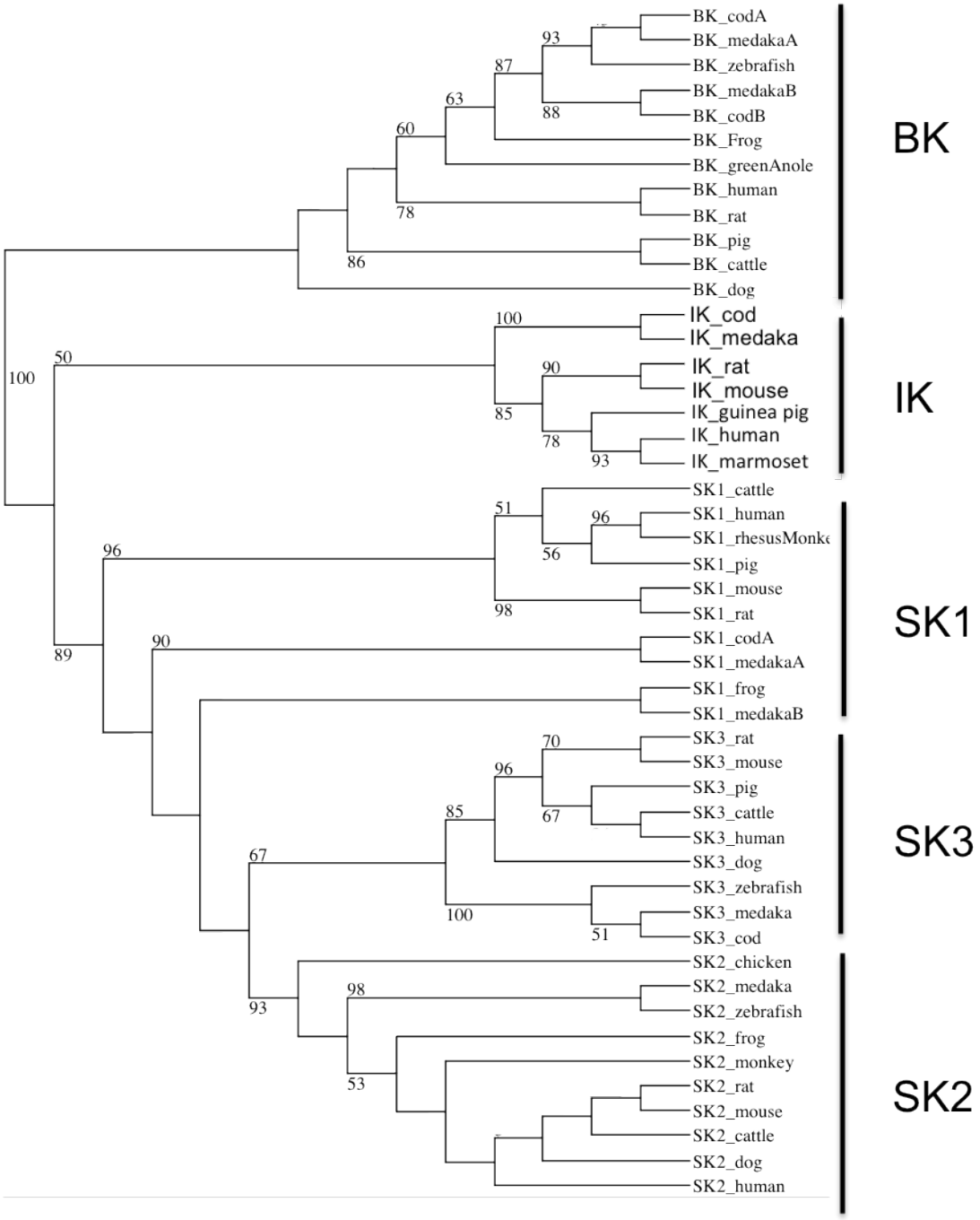

Figure 34 K_{Ca} channel phylogenetic tree. Phylogenetic tree constructed as in figure 29. The tree branches off in two clads, where one clad consists of the BK potassium channel and the other clad consisting of IK and the three SK channels. Thereby the tree branches off with IK in one clad and the three SK-channels in another. The SK channels share similar features, but the phylogenetic relationship show that they are different from each other. The eel-sequence was removed before this analysis, because it was only partially obtained and therefore made the phylogenetic analysis difficult. All gene accession numbers could be found in Appendix 1.

4 Discussion of methods

4.1 Genotyping

All fish included in the study were genotyped to ensure that all sampled individuals were females. Even though the females were picked out based on phenotype at a low error rate, it was slightly more difficult to discriminate between sexes in the juveniles than the adults. This is because the juveniles are of small size and the sex characteristics are less apparent. When studying gene expression differences between two conditions (e.g. juveniles and adults) it is important to ensure that possible differences between the samples are due to the variable that is intended to study, and not other variables e.g. sex-differences.

For genotyping, we used primers and protocol proposed by Shinomiya et al (2004). These primers should amplify both the somatic DMRT1 gene and the male-specific DMY gene. However, the protocol had to be optimized to amplify the genes in our lab. We tested and optimized protocols for both DNA isolation and for PCR amplification. For DNA isolation different homogenization protocols and incubation on water bath (time and temperature) were tested, and for PCR amplification different concentrations of $MgCl_2$ were tested as well as different PCR programs. The PCR program that was used was a touchdown program, where the annealing temperature dropped one centigrade per cycle, because the two primers had different melting temperatures (64.4 ˚C and 73.0 ˚C). It was surprising that the band for the amplified autosomal DMRT1gene in males was not obtained despite the optimization of the protocol. However the primers were originally designed for the Hd-rR strain, which is slightly different from the d-rR strain that was used in this project (Shinomiya et al 2004). Despite lacking the somatic band in males, the difference in size between DMY and DMRT1 was sufficiently distinct to separate the sexes, so it was not investigated further.

4.2 Optimization of FACS-sorting

The FACS sorting was thoroughly tested before it was performed on the genotyped samples, as should all new cell types sorted with FACS for the first time (Tzur et al 2011). The testing was performed to find the conditions that gave a homogenous population of healthy cells. It was tested several types of media, to increase the survival of the cells. During testing we discovered that keeping the cells in EC medium during sorting increased the survival of the cells. The sorting was also tested with and without APC, without APC only the dead cells were sorted out. Since we suspected that apoptotic cells could interfere with the analysis, we chose to stain with APC to discard apoptotic cells with a high degree of certainty.

4.3 RNA-seq

The quality of the RNA-seq experiment was overall very good, and thus regarded successful. Due to the small amount of RNA obtained from the juveniles, Ovation RNA Seq System V2 (NuGEN) designed for pre-amplification of RNA samples before RNA-seq was used. This may introduce bias in the sample before RNA-seq, but according to the manufacturer this should not happen. However, we pre-amplified the adult sample also, so that the samples were treated equally.

In the version of the medaka genome that is available, there are many genes that are not annotated since they were reported after the genome was published. Consequently some genes are missed in the present analysis and must be manually searched for if they are of interest, which take time. E.g. the kiss receptors were annotated after the medaka genome was published, so the receptors must be manually searched for to find out the expression of this channel. Some groups have planned to work on re-annotating the medaka genome. When the new genome becomes available, the improved annotation will help the discovery of more genes and our material will be mapped again.

Since we mapped the reads only to the part of the genome assembled in chromosomes, genes were also missed if they were located on parts assembled in scaffolds. To know what genes that that are assembled in the scaffolds, each gene have to be searched for manually. Therefore, genes that are expressed in neither adult nor juvenile are difficult to analyse. Thus, our group will map the reads again and this time include the scaffolds in addition to chromosomes in the mapping, so the genes that are located on scaffolds also will be found. Only then, we can be sure if the genes are expressed or not in the LH-producing gonadotropes.

Also, there are some general drawbacks that should be considered when interpreting RNA-seq data. One of the drawbacks is that the huge amount of data could be hard to handle and analyse without the necessary bioinformatics skills. The sequencing error rate for NGS is much higher than for more traditional approaches such as Sanger sequencing, so the interpretation of the data should be considered carefully (Kircher & Kelso 2010). Also, the relatively high error rate could make it challenging to separate SNP (single nucleotide polymorphism) from the sequencing errors. However, a higher sequencing depth (how many times a base is covered) could reduce the error rate (Li et al. 2009). RNA-seq is still one of the best tools available for exploring the transcriptome, especially since RNA-seq offers the opportunity to study transcriptome of species without a sequenced genome.

The data analysis indeed proved to be more challenging than intended, demanding more knowledge in bioinformatics as well as more time than first thought. One of the main challenges with the HTS-technology is that a lot of sequence information is easily obtained, but the analyses of the material are demanding (Ozsolak & Milos 2010).

4.4 K_{Ca} channel sequences

4.4.1 Isolation of eel, cod and medaka K_{Ca} sequences

Parts of the published cod genome were not completely resolved due to sequencing difficulties (Star et al 2011). In some areas of the one variant of the SK1 channel sequences, the cod sequence had a gap that made it necessary to remove the particular cod sequence from the tree analysis.

I was not able to find the SK3 and IK channel sequences from eel by searching the eel genome (Henkel et al, 2012). This could be due to the large similarities between the sequence of SK1-3 and IK, thus making it difficult to find blast sequences that discriminated the channels, or that I partly used the sequenced pituitary transcriptome to search for K_{Ca} channels sequences in the eel, and that these channels were not expressed in the pituitary of eel at the sampling time. Also the eel genome is only recently sequenced, and is not necessarily complete. It seemed that all the eel sequences were only partially obtained by searching the genome and the pituitary transcriptome, and it would have been interesting to find the remaining sequence of the channels obtained and the two channels that was not obtained by cloning.

Some of the sequence could be out of the reading frame, since missing exon-intron boundary by only one base could have shifted the reading frame. I found the reading frame that contained the GYGD-sequence since this is the signature sequence of the K_{Ca} channels; I also searched for other known protein sequences. However, I could have split the DNA sequence in more parts, and searched the different part of the DNA sequence for reading frames separately, and perhaps more of the amino acid sequence could have been obtained.

4.4.2 Constructing the phylogenetic trees

Alignments were tested with the program ProtTest (bioportal.uio.no) (Abascal et al 2005) to find the best fitted evolutionary model with improvements to the evolutionary models. However, it was not possible to implement all the improvement of the models in SeaView 4.3.3 (Gouy, 2010). SeaView 4.3.3 was run locally on the computer, and used many days to construct the trees. The output from SeaView 4.3.3 is in PDF (portable document format), which is a format that is difficult to process. There exist other alternatives to SeaView 4.3.3 such as EnsemblCompara GeneTrees (Vilella et al. 2009), which are performed online at Ensembl, and is a pipeline where the whole procedure is performed in the same resource.

Since such a small part of the eel sequence was obtained, the analysis was performed on very similar sequences; the relationship among the branches of the tree may therefore be a bit obstructed. It may have improved the quality of the phylogenetic analyses to use sequences from additional teleost species for more information about the evolutionary relationship among the channels, but unfortunately many of the teleost K_{Ca} channel sequences in the public databases are only partially obtained.

5 Discussion of results

In this study the transcriptome of the LH-producing gonadotropes of juvenile and adult female medaka has been sequenced with RNA-seq. I focused on the expression of some genes known to be involved in puberty, GnRH-Rs, the LHβ-subunit and dopamine receptors, since there was not time to investigate all the sequenced material.

This study also focused on the K_{Ca} channels, and reports expression of all the K_{Ca} channels variants in the LH-producing gonadotropes, except for one of the SK1-variants. Furthermore, K_{Ca} channel sequences have been identified in eel, medaka and cod. In cod and medaka, two variants of the SK1 and BK channel sequences were obtained. In eel, only the BK, SK1 and SK2 channel sequences were obtained, and no evidence of two variants of the same channel type was found. The phylogenetic relationship among the K_{Ca} channel sequences has been investigated. The phylogenetic tree combining all the K_{Ca} channel types displayed the expected relationship between the channel groups, the SK and IK channels being more similar to each other, than to the BK channels.

5.1 RNA seq

Carter (2006) proposed that cellular transcriptomics would be the next phase of endocrine profiling. However, there is currently little information available about RNA-seq on defined pituitary cells. Reported transcriptome studies are mostly based on whole-pituitary samples and thus it is difficult to compare to this study that is performed on defined LH cells.

I chose to focus on the expression of the genes for the GnRH-Rs, the LHβ and the dopamine receptors, in addition to the K_{Ca} channels (described in 5.2), as they should be central in the regulation of puberty. I expected to find expression of GnRH-R mRNA, and that the expression would be higher in the adult sample as qPCR of GnRH-Rs in female striped bass showed that it was a significant increase in GnRH-R from previtellogenic fish to mature fish (..Alok, 2000). The measured intensity of GFP-expression in FACS was higher in the adult cells than cells from juveniles. It was therefore expected to find LHβ mRNA in both juveniles and adults, but that the adult sample would express more LHβ mRNA, since the expression of LHβ and GFP is controlled by the same promoter. The D_2 receptor is known to be involved in the inhibition of LH secretion in goldfish (..Chang,1990), thus it was expected to be expressed in the medaka LH-producing gonadotropes as well.

The count of the GnRH-R3 expression was very low in the adult sample, and no expression was detected in the juveniles. No evidence was found for the expression of other GnRH-Rs. This does not mean that they are not expressed in the LH-producing gonadotropes, as they are located on the part of the genome that is assembled in scaffolds. Due to the very low expression of GnRH-R3, I would expect one or more additional GnRH-R to be expressed, since GnRH is important for the function of LH cells (for review see Yaron, 2003). The expression of LHβ-mRNA was high in both juvenile and adult cells, as expected. Surprisingly, the expression of LHβ-mRNA was slightly higher in the juveniles than the adults, while the opposite was expected. LH has been shown to be more important in the end of maturation than in the beginning, and is involved in reproductive activity. However, the

number of LH cells was considerably higher in the adult pituitary, and this indicates that LH is more important in adults than juveniles. Expression of three different dopamine receptors D_1, D_2 and D_3 were found. D_1 and D_3 showed a higher expression in juveniles than in adults, and also had a greater fold change than the D_2 receptor, which showed a slightly higher expression in adults than in juveniles. Dopamine is known to inhibit secretion of LH through the D_2 receptor (for review see Zohar, 2010).

In the hundred most differentially expressed genes between juveniles and adults presented in figure 22, there were no genes immediately recognized as having a known function in puberty. However, it was not time in this master thesis to analyse the individual genes further.

5.2 Analysis of the K_{Ca} channels

The K_{Ca} channel sequences were obtained from eel, cod and medaka by searching their respective genomes. Then the K_{Ca} channel sequences were compared by phylogenetic analysis to see if the channel sequences obtained were related to the corresponding channel sequences of other organisms, and to see the relationship among the different channel types. It is important to study the K_{Ca} channels closer, due to the assumed role in the signalling pathway that regulates hormone secretion in gonadotropes of teleost fish.

5.2.1 Expression of K_{Ca} channels in gonadotropes

In several organisms there is evidence of K_{Ca} channels being present in gonadotropes (Heyward et al 1995; Hodne et al, unpublished; Kukuljan et al 1992; Tse & Hille 1992; Waring & Turgeon 2009), and it was expected to find transcripts of these channels also in the LH- gonadotropes of female medaka. In rat gonadotropes studied with the patch-clamp technique, the SK channels were the main K_{Ca} channel type (Stojilkovic et al 2005). In cod, FSH-gonadotropes seem to have mostly BK-channels, while LH-gonadotropes have mainly SK channels (Hodne et al, unpublished). However, in mouse gonadotropes, both BK and SK channels were present, and GnRH stimulation increased the BK channel current (Waring & Turgeon 2009). Due to the varying evidence of the main expressed channel type in the different pituitary cell types, it was not possible to expect which channel type that was more expressed.

The RNA-seq results regarding the K_{Ca} channels proved that mRNA for all the channel types is expressed in LH-producing gonadotropes in both juvenile and adult female medaka. The two BK channel types seemed to be more highly expressed than the SK-channels. The composition of SK and BK channels in a cell may affect the control of secretion, and thus will be interesting to explore further (Stojilkovic et al 2005; Waring & Turgeon 2009). Although it seemed to be more BK channel expression than SK channel expression in the medaka LH-producing gonadotropes, however, a difference in mRNA expression does not necessarily reflect differences at protein level, due to half-life, translation rates of the mRNA and modulation and degradation rate of the translated protein (Greenbaum et al. 2003).

5.2.2 Phylogenetic tree analyses

The part of the eel channel sequences obtained, was found to be similar to the other teleosts species in the area where the eel channel sequence probably was genuine. I therefore expected the eel channel sequence to relate to the other teleost channel sequences. I also expected the eel to branch of earlier than the other teleosts, reflecting that eel is a more primitive type of teleost than medaka and cod (Inoue et al. 2003).

In the phylogenetic tree of the BK channels, the eel channel branched off earlier than the other teleosts, as expected. For the other channels the eel sequences did not branch off earlier, but was found in the branch that contained the other teleost fish. In the combined analysis of all the K_{Ca} channel sequences, a longer stretch of the BK channel sequence was included, and the relationship among the cod and medaka channels changed, probably due to the fact that the sequences were less similar in the sections that were not included in the phylogenetic tree of only the BK channels. As expected the A sequences of cod and medaka was more related, than to the B sequence of the same species. The changed relationship when including more of the sequence as seen in the BK channel analysis, may also explain why all the eel channels, except from the BK channel, did not branch of earlier than the other teleosts channel sequences as expected, since the small part of eel sequence obtained, showed a high similarity in all species.

According to Rohmann (2009) most teleosts have two BK variants; in medaka LH-gonadotropes both variants were expressed. Also, in cod two variants of BK was found, as well as two variants of the SK1 gene in both cod and medaka. In eel, only one version of each channel type was found, and this may indicate that the eel only got one version. However, since I was not able to obtain all the K_{Ca} channel sequences from the eel genome, it could mean that also more variants of the channels exist.

For the gene SK1, one of the variants from cod and medaka branched off earlier than the others, and were undoubtedly different from all the other SK sequences. Since this particular variant also was not expressed in the LH-producing gonadotropes of medaka, this may indicate that the channel is a pseudo-variant and a non-functional remnant from the whole-genome duplication event (Hoegg et al 2004). Since the cod sequence variant was very similar to that of medaka, this may also be the case of the cod variant. It could however, also mean that the variant was not expressed in the pituitary.

Phylogenetic tree analysis comprising of all channels (except for the obtained eel sequences), branched off with the BK channels in one clad, and the other clad consisting of the SK channels and IK channels reflecting the relationship among the channels, the SK and IK channels being structurally more similar than the BK channel. (For reviews see Stocker 2004; Wei et al 2005). Also, the cod and medaka channel sequences were found in the expected clads, supporting that the sequences I obtained were genuine channel sequences.

5.3 Conclusion

In conclusion, the transcriptome of LH-producing gonadotropes has been profiled in this study. I focused on genes known to be involved in reproduction, and found the expression levels of GnRH-R's, the LHβ and the dopamine receptors. All the K_{Ca} channel sequences,

except for one SK1 variant, were expressed in the LH cells. K_{Ca} channel sequences have been obtained from eel, cod and medaka. Two versions of both BK- and SK1 channel were found in both medaka and cod. However, the SK1 gene seemed to be non-functional as it was the only version not expressed in gonadotropes, and also was phylogenetically different from the other SK1 channel sequences. In eel, partial sequences of the BK, SK1 and SK2 channel were obtained. Phylogenetic analyses K_{Ca} channel sequences have been conducted, and the channels showed the relationship as expected according to channel type and between species.

6 Future work

Two additional samples from both juvenile and adult medaka were recently sequenced by Illumina with comparable quality and a higher number of reads than for the samples described in this project. The new samples will be mapped to the whole genome, including the part presently assembled in scaffolds. Increasing the number of replicates for each reproductive stage from one to three will improve the robustness of the data. Analysis of these data will be performed soon, as well as analyses of the differential gene expression obtained in this project.

Our group is currently developing a (fshb:GFP) transgenic line of medaka, it will be of great interest to use RNA-seq to study the FSH-producing gonadotropes and compare them to the expression results obtained in this study. Our group has found clear functional differences between FSH and LH cells in cod gonadotropes including differential expression of K_{Ca} channels (Hodne et al, unpublished), and it would therefore be of great interest to see if the same holds true for medaka. Furthermore it would be interesting to conduct the same analysis with males for both LH- and FSH-producing gonadotropes to see if there are differences between the sexes.

Gene expression of the LH-producing gonadotropes could be compared with patch-clamping studies of the same gonadotropes upon stimulation with GnRH, to see how the K_{Ca} channels are involved in secretion control.

7 References

Abascal F, Zardoya R, Posada D. 2005. ProtTest: selection of best-fit models of protein evolution. *Bioinformatics* 21: 2104-05

Alok D, Hassin S, Sampath Kumar R, Trant JM, Yu K, Zohar Y. 2000. Characterization of a pituitary GnRH-receptor from a perciform fish, Morone saxatilis: functional expression in a fish cell line. *Molecular and cellular endocrinology* 168: 65-75

Amano M, Aida K, Okumoto N, Hasegawa Y. 1992. Changes in Salmon GnRH and Chicken GnRH-II Contents in the Brain and Pituitary, and GTH Contents in the Pituitary in Female Masu Salmon, Oncorhynchus masou, from Hatching through Ovulation (Endocrinology). *Zoological science* 9: 375-86

Bao L, Kaldany C, Holmstrand EC, Cox DH. 2004. Mapping the BKCa Channel's "Ca2+ Bowl". *The Journal of general physiology* 123: 475-89

Begenisich T, Nakamoto T, Ovitt CE, Nehrke K, Brugnara C, Alper SL, Melvin JE. 2004. Physiological roles of the intermediate conductance, Ca2+-activated potassium channel Kcnn4. *Journal of Biological Chemistry* 279: 47681-87

Beisel KW, Rocha-Sanchez SM, Ziegenbein SJ, Morris KA, Kai C, Kawai J, Carninci P, Hayashizaki Y, Davis RL. 2007. Diversity of Ca 2+-activated K+ channel transcripts in inner ear hair cells. *Gene* 386: 11-23

Berg Vaule S. 2011. *Molecular characterization and gene expression analysis of calcium-activated potassium channels in Atlantic cod (Gadus morhua)*
University of Oslo, Oslo

Berkefeld H, Sailer CA, Bildl W, Rohde V, Thumfart JO, Eble S, Klugbauer N, Reisinger E, Bischofberger J, Oliver D. 2006. BKCa-Cav channel complexes mediate rapid and localized Ca2+-activated K+ signaling. *Science's STKE* 314: 615

Bromage N, Porter M, Randall C. 2001. The environmental regulation of maturation in farmed finfish with special reference to the role of photoperiod and melatonin. *Aquaculture* 197: 63-98

Carter D. 2006. Cellular transcriptomics–the next phase of endocrine expression profiling. *Trends in Endocrinology & Metabolism* 17: 192-98

Chang JP, Cook H, Freedman GL, Jim Wiggs A, Somoza GM, de Leeuw R, Peter RE. 1990. Use of a pituitary cell dispersion method and primary culture system for the studies of gonadotropin-releasing hormone action in the goldfish, Carassius auratus I. Initial morphological, static, and cell column perifusion studies. *General and comparative endocrinology* 77: 256-73

Chang JP, Johnson JD, Sawisky GR, Grey CL, Mitchell G, Booth M, Volk MM, Parks SK, Thompson E, Goss GG. 2009. Signal transduction in multifactorial neuroendocrine control of gonadotropin secretion and synthesis in teleosts--studies on the goldfish model. *General and comparative endocrinology* 161: 42-52

Cloonan N, Grimmond SM. 2008. Transcriptome content and dynamics at single-nucleotide resolution. *Genome biology* 9: 234

De Leeuw R, Van't Veer C, Goos H, Van Oordt P. 1988. The dopaminergic regulation of gonadotropin-releasing hormone receptor binding in the pituitary of the African catfish, Clarias gariepinus. *General and comparative endocrinology* 72: 408-15

Dick GM, Sanders KM. 2001. (Xeno) estrogen Sensitivity of Smooth Muscle BK Channels Conferred by the Regulatory β1 Subunit A STUDY OF β1 KNOCKOUT MICE. *Journal of Biological Chemistry* 276: 44835-40

Dufour S, Burzawa-Gérard E, Le Belle N, Sbaihi M, Vidal B. 2003. Reproductive endocrinology of the European eel, Anguilla anguilla. *Eel Biology. Tokyo, Springer*: 373-83

Edgar RC. 2004. MUSCLE: multiple sequence alignment with high accuracy and high throughput. *Nucleic acids research* 32: 1792-97

Fettiplace R, Fuchs P. 1999. Mechanisms of hair cell tuning. *Annual review of physiology* 61: 809-34

Filby AL, van Aerle R, Duitman JW, Tyler CR. 2008. The kisspeptin/gonadotropin-releasing hormone pathway and molecular signaling of puberty in fish. *Biology of reproduction* 78: 278-89

Gouy M, Guindon S, Gascuel O. 2010. SeaView version 4: a multiplatform graphical user interface for sequence alignment and phylogenetic tree building. *Molecular biology and evolution* 27: 221-24

Greenbaum D, Colangelo C, Williams K, Gerstein M. 2003. Comparing protein abundance and mRNA expression levels on a genomic scale. *Genome Biol* 4: 117

Hassin S, Claire M, Holland H, Zohar Y. 1999. Ontogeny of follicle-stimulating hormone and luteinizing hormone gene expression during pubertal development in the female striped bass, Morone saxatilis (Teleostei). *Biology of reproduction* 61: 1608-15

Hassin S, Gothilf Y, Blaise O, Zohar Y. 1998. Gonadotropin-I and-II subunit gene expression of male striped bass (Morone saxatilis) after gonadotropin-releasing hormone analogue injection: quantitation using an optimized ribonuclease protection assay. *Biology of reproduction* 58: 1233-40

Haug T, Hafting T, Sand O. 2004. Inhibition of BK channels contributes to the second phase of the response to TRH in clonal rat anterior pituitary cells. *Acta physiologica scandinavica* 180: 347-57

Haug TM, Hodne K, Weltzien FA, Sand O. 2007. Electrophysiological Properties of Pituitary Cells in Primary Culture from Atlantic Cod< i>(Gadus morhua)</i>. *Neuroendocrinology* 86: 38-47

Henkel CV, Burgerhout E, de Wijze DL, Dirks RP, Minegishi Y, Jansen HJ, Spaink HP, Dufour S, Weltzien FA, Tsukamoto K, Guido E. E. J. M. van den Thillart 2012. Primitive Duplicate Hox Clusters in the European Eel's Genome. *PloS one* 7: e32231

Heyward P, Chen C, Clarke I. 1995. Inward membrane currents and electrophysiological responses to GnRH in ovine gonadotropes. *Neuroendocrinology* 61: 609-21

Hildahl J, Sandvik GK, Edvardsen RB, Norberg B, Haug TM, Weltzien FA. 2011. Four gonadotropin releasing hormone receptor genes in Atlantic cod are differentially expressed in the brain and pituitary during puberty. *General and comparative endocrinology*

Hoegg S, Brinkmann H, Taylor JS, Meyer A. 2004. Phylogenetic timing of the fish-specific genome duplication correlates with the diversification of teleost fish. *Journal of molecular evolution* 59: 190-203

Hoffman JF, Joiner W, Nehrke K, Potapova O, Foye K, Wickrema A. 2003. The hSK4 (KCNN4) isoform is the Ca2+-activated K+ channel (Gardos channel) in human red blood cells. *Proceedings of the National Academy of Sciences* 100: 7366

Holland M, Hassin S, Zohar Y. 2001. Seasonal fluctuations in pituitary levels of the three forms of gonadotropin-releasing hormone in striped bass, Morone saxatilis (Teleostei), during juvenile and pubertal development. *Journal of endocrinology* 169: 527-38

Ibrahim S, van den Engh G. 2007. Flow cytometry and cell sorting. *Cell Separation*: 19-39

Inoue JG, Miya M, Tsukamoto K, Nishida M. 2003. Basal actinopterygian relationships: a mitogenomic perspective on the phylogeny of the. *Molecular phylogenetics and evolution* 26: 110-20

Kah O, Dubough P, Martinoli MG, Rabhi M, Gonnet F, Geffard M, Calas A. 1987. Central GABAergic innervation of the pituitary in goldfish: a radioautographic and immunocytochemical study at the electron microscope level. *General and comparative endocrinology* 67: 324-32

Kah O, Peter RE, Dubourg P, Cook H. 1983. Effects of monosodium-glutamate on pituitary innervation in goldfish, Carassius auratus. *General and comparative endocrinology* 51: 338-46

Kanda S, Akazome Y, Matsunaga T, Yamamoto N, Yamada S, Tsukamura H, Maeda K, Oka Y. 2008. Identification of KiSS-1 product kisspeptin and steroid-sensitive sexually dimorphic kisspeptin neurons in medaka (Oryzias latipes). *Endocrinology* 149: 2467-76

Kandel-Kfir M, Gur G, Melamed P, Zilberstein Y, Cohen Y, Zmora N, Kobayashi M, Elizur A, Yaron Z. 2002. Gonadotropin response to GnRH during sexual ontogeny in the common carp, Cyprinus carpio. *Comparative Biochemistry and Physiology Part B: Biochemistry and Molecular Biology* 132: 17-26

Kaneko T, Hirano T. 1993. Role of prolactin and somatolactin in calcium regulation in fish. *Journal of experimental biology* 184: 31-45

Karlsen Ø, Norberg B, Kjesbu O, Taranger G. 2006. Effects of photoperiod and exercise on growth, liver size, and age at puberty in farmed Atlantic cod (Gadus morhua L.). *ICES Journal of Marine Science: Journal du Conseil* 63: 355-64

Kasahara M, Naruse K, Sasaki S, Nakatani Y, Qu W, Ahsan B, Yamada T, Nagayasu Y, Doi K, Kasai Y, Jindo T, Kobayashi D, Shimada A, Toyoda A, Kuroki Y, Fujiyama A, Sasaki T, Shimizu A, Asakawa S, Shimizu N, Hashimoto S-i, Yang J, Lee Y, Matsushima K, Sugano S, Sakaizumi M, Narita T, Ohishi K, Haga S, Ohta F, Nomoto H, Nogata K, Morishita T, Endo T, Shin-I T, Takeda H, Morishita S, Kohara Y. 2007. The medaka draft genome and insights into vertebrate genome evolution. *Nature* 447: 714-19

Kim J, Hoffman DA. 2008. Potassium channels: newly found players in synaptic plasticity. *The Neuroscientist* 14: 276-86

Kircher M, Kelso J. 2010. High‐throughput DNA sequencing–concepts and limitations. *Bioessays* 32: 524-36

Kitahashi T, Ogawa S, Parhar IS. 2009. Cloning and expression of kiss2 in the zebrafish and medaka. *Endocrinology* 150: 821-31

Knaus HG, Folander K, Garcia-Calvo M, Garcia ML, Kaczorowski GJ, Smith M, Swanson R. 1994. Primary sequence and immunological characterization of beta-subunit of high conductance Ca (2+)-activated K+ channel from smooth muscle. *Journal of Biological Chemistry* 269: 17274-78

Kondo M, Nanda I, Schmid M, Schartl M. 2009. Sex determination and sex chromosome evolution: insights from medaka. *Sexual Development* 3: 88-98

Korovkina VP, Brainard AM, Ismail P, Schmidt TJ, England SK. 2004. Estradiol binding to maxi-K channels induces their down-regulation via proteasomal degradation. *Journal of Biological Chemistry* 279: 1217-23

Kukuljan M, Stojilkovic SS, Rojas E, Catt KJ. 1992. Apamin-sensitive potassium channels mediate agonist-induced oscillations of membrane potential in pituitary gonadotrophs. *FEBS letters* 301: 19-22

Köhler M, Hirschberg B, Bond C, Kinzie J, Marrion N, Maylie J, Adelman J. 1996. Small-conductance, calcium-activated potassium channels from mammalian brain. *Science* 273: 1709

Latorre R, Oberhauser A, Labarca P, Alvarez O. 1989. Varieties of calcium-activated potassium channels. *Annual review of physiology* 51: 385-99

Le Cam A, Bobe J, Bouchez O, Cabeau C, Kah O, Klopp C, Lareyre JJ, Le Guen I, Lluch J, Montfort J. 2012. Characterization of rainbow trout gonad, brain and gill deep cDNA repertoires using a Roche 454-Titanium sequencing approach. *Gene*

Ledoux J, Werner ME, Brayden JE, Nelson MT. 2006. Calcium-activated potassium channels and the regulation of vascular tone. *Physiology (Bethesda, Md.)* 21: 69

Levavi-Sivan B, Bogerd J, Mañanós EL, Gómez A, Lareyre JJ. 2010. Perspectives on fish gonadotropins and their receptors. *General and comparative endocrinology* 165: 412-37

Li H, Handsaker B, Wysoker A, Fennell T, Ruan J, Homer N, Marth G, Abecasis G, Durbin R. 2009. The sequence alignment/map format and SAMtools. *Bioinformatics* 25: 2078-79

Lionetto MG, Rizzello A, Giordano ME, Maffia M, De Nuccio F, Nicolardi G, Hoffmann EK, Schettino T. 2008. Molecular and Functional Expression of High Conductance Ca 2+ Activated K+ Channels in the Eel Intestinal Epithelium. *Cellular Physiology and Biochemistry* 21: 373-84

Madigou T, Mañanos-Sanchez E, Hulshof S, Anglade I, Zanuy S, Kah O. 2000. Cloning, tissue distribution, and central expression of the gonadotropin-releasing hormone receptor in the rainbow trout (Oncorhynchus mykiss). *Biology of reproduction* 63: 1857-66

Marguerat S, Bähler J. 2010. RNA-seq: from technology to biology. *Cellular and molecular life sciences* 67: 569-79

Martin JA, Wang Z. 2011. Next-generation transcriptome assembly. *Nature Reviews Genetics* 12: 671-82

McClure CA, Hammell KL, Moore M, Dohoo IR, Burnley H. 2007. Risk factors for early sexual maturation in Atlantic salmon in seawater farms in New Brunswick and Nova Scotia, Canada. *Aquaculture* 272: 370-79

Meera P, Wallner M, Song M, Toro L. 1997. Large conductance voltage-and calcium-dependent K+ channel, a distinct member of voltage-dependent ion channels with seven N-terminal transmembrane segments (S0-S6), an extracellular N terminus, and an intracellular (S9-S10) C terminus. *Proceedings of the National Academy of Sciences* 94: 14066

Meera P, Wallner M, Toro L. 2000. A neuronal β subunit (KCNMB4) makes the large conductance, voltage-and Ca2+-activated K+ channel resistant to charybdotoxin and iberiotoxin. *Proceedings of the National Academy of Sciences* 97: 5562

Miwa S, Yan L, Swanson P. 1994. Localization of two gonadotropin receptors in the salmon gonad by in vitro ligand autoradiography. *Biology of reproduction* 50: 629-42

Mongan L, Hill M, Chen M, Tate S, Collins S, Buckby L, Grubb B. 2005. The distribution of small and intermediate conductance calcium-activated potassium channels in the rat sensory nervous system. *Neuroscience* 131: 161-75

Mortazavi A, Williams BA, McCue K, Schaeffer L, Wold B. 2008. Mapping and quantifying mammalian transcriptomes by RNA-Seq. *Nature methods* 5: 621-28

Mørk H, Haug T, Sand O. 2005. Contribution of different Ca2+ ‐ activated K+ channels to the first phase of the response to TRH in clonal rat anterior pituitary cells. *Acta physiologica scandinavica* 184: 141-50

Norris D. 1997. *Vertebrate endocrinology*. San Diego: Academic press.

Okada T, Kawazoe I, Kimura S, Sasamoto Y, Aida K, Kawauchi H. 1994. Purification and characterization of gonadotropin I and II from pituitary glands of tuna (Thunnus obesus). *International Journal of Peptide and Protein Research* 43: 69-80

Okubo K, Nagahama Y. 2008. Structural and functional evolution of gonadotropin‐releasing hormone in vertebrates. *Acta Physiologica* 193: 3-15

Okubo K, Nagata S, Ko R, Kataoka H, Yoshiura Y, Mitani H, Kondo M, Naruse K, Shima A, Aida K. 2001. Identification and characterization of two distinct GnRH receptor subtypes in a teleost, the medaka Oryzias latipes. *Endocrinology* 142: 4729-39

Okubo K, Suetake H, Usami T, Aida K. 2000. Molecular cloning and tissue-specific expression of a gonadotropin-releasing hormone receptor in the Japanese eel. *General and comparative endocrinology* 119: 181-92

Okuzawa K. 2002. Puberty in teleosts. *Fish Physiology and Biochemistry* 26: 31-41

Orio P, Rojas P, Ferreira G, Latorre R. 2002. New disguises for an old channel: MaxiK channel beta-subunits. *News in physiological sciences: an international journal of physiology produced jointly by the International Union of Physiological Sciences and the American Physiological Society* 17: 156

Ouadid-Ahidouch H, Chaussade F, Roudbaraki M, Slomianny C, Dewailly E, Delcourt P, Prevarskaya N. 2000. KV1. 1 K+ Channels Identification in Human Breast Carcinoma Cells: Involvement in Cell Proliferation. *Biochemical and biophysical research communications* 278: 272-77

Ozawa S, Sand O. 1986. Electrophysiology of excitable endocrine cells. *Physiological reviews* 66: 887-952

Ozsolak F, Milos PM. 2010. RNA sequencing: advances, challenges and opportunities. *Nature Reviews Genetics* 12: 87-98

Pasquier J, Lafont AG, Leprince J, Vaudry H, Rousseau K, Dufour S. 2011. First evidence for a direct inhibitory effect of kisspeptins on LH expression in the eel, Anguilla anguilla. *General and comparative endocrinology*

Petersen OH, Maruyama Y. 1984. Calcium-activated potassium channels and their role in secretion. *Nature* 307: 693

Prat F, Sumpter JP, Tyler CR. 1996. Validation of radioimmunoassays for two salmon gonadotropins (GTH I and GTH II) and their plasma concentrations throughout the reproductivecycle in male and female rainbow trout (Oncorhynchus mykiss). *Biology of reproduction* 54: 1375-82

Revel FG, Saboureau M, Masson-Pévet M, Pévet P, Mikkelsen JD, Simonneaux V. 2006. Kisspeptin mediates the photoperiodic control of reproduction in hamsters. *Current biology* 16: 1730-35

Roa J, Tena-Sempere M. 2007. KiSS-1 system and reproduction: comparative aspects and roles in the control of female gonadotropic axis in mammals. *General and comparative endocrinology* 153: 132-40

Rohmann KN, Deitcher DL, Bass AH. 2009. Calcium-activated potassium (BK) channels are encoded by duplicate slo1 genes in teleost fishes. *Molecular biology and evolution* 26: 1509-21

Romano LA, Loretz CA, Fourtner CR. 1996. Potassium channels in pituitary cells in the teleost, Gillichthys mirabilis. *Comparative Biochemistry and Physiology Part A: Physiology* 113: 143-56

Sabban S. 2011. Development of an in vitro model system for studying the interaction of Equus caballus IgE with its high-affinity FcεRI receptor.

Saeed AI, Bhagabati NK, Braisted JC, Liang W, Sharov V, Howe EA, Li J, Thiagarajan M, White JA, Quackenbush J. 2006. [9] TM4 Microarray Software Suite. *Methods in enzymology* 411: 134-93

Sah P. 1996. Ca< sup> 2+</sup>-activated K< sup>+</sup> currents in neurones: types, physiological roles and modulation. *Trends in neurosciences* 19: 150-54

Sawada K, Ukena K, Satake H, Iwakoshi E, Minakata H, Tsutsui K. 2002. Novel fish hypothalamic neuropeptide. *European Journal of Biochemistry* 269: 6000-08

Schulz RW, Goos HJT. 1999. Puberty in male fish: concepts and recent developments with special reference to the African catfish (Clarias gariepinus). *Aquaculture* 177: 5-12

Schumacher MA, Rivard AF, Bächinger HP, Adelman JP. 2001. Structure of the gating domain of a Ca2plus;-activated Kplus; channel complexed with Ca2plus;/calmodulin. *Nature* 410: 1120-24

Schwab A. 2001. Function and spatial distribution of ion channels and transporters in cell migration. *American Journal of Physiology-Renal Physiology* 280: F739-F47

Sendler E, Johnson GD, Krawetz SA. 2011. Local and global factors affecting RNAseq analysis. *Analytical biochemistry*

Shinomiya A, Otake H, Togashi K, Hamaguchi S, Sakaizumi M. 2004. Field survey of sex-reversals in the medaka, Oryzias latipes: genotypic sexing of wild populations. *Zoological science* 21: 613-19

So WK, Kwok HF, Ge W. 2005. Zebrafish gonadotropins and their receptors: II. Cloning and characterization of zebrafish follicle-stimulating hormone and luteinizing hormone subunits—their spatial-temporal expression patterns and receptor specificity. *Biology of reproduction* 72: 1382-96

Star B, Nederbragt AJ, Jentoft S, Grimholt U, Malmstrøm M, Gregers TF, Rounge TB, Paulsen J, Solbakken MH, Sharma A. 2011. The genome sequence of Atlantic cod reveals a unique immune system. *Nature* 477: 207-10

Stocker M. 2004. Ca2+-activated K+ channels: molecular determinants and function of the SK family. *Nature Reviews Neuroscience* 5: 758-70

Stocker M, Krause M, Pedarzani P. 1999. An apamin-sensitive Ca2+-activated K+ current in hippocampal pyramidal neurons. *Proceedings of the National Academy of Sciences* 96: 4662

Stocker M, Pedarzani P. 2000. Differential distribution of three Ca2+-activated K+ channel subunits, SK1, SK2, and SK3, in the adult rat central nervous system. *Molecular and Cellular Neuroscience* 15: 476-93

Stojilkovic SS, Zemkova H, Van Goor F. 2005. Biophysical basis of pituitary cell type-specific Ca< sup> 2+</sup> signaling–secretion coupling. *Trends in Endocrinology & Metabolism* 16: 152-59

Su AI, Cooke MP, Ching KA, Hakak Y, Walker JR, Wiltshire T, Orth AP, Vega RG, Sapinoso LM, Moqrich A. 2002. Large-scale analysis of the human and mouse transcriptomes. *Proceedings of the National Academy of Sciences* 99: 4465

Tacconi S, Carletti R, Bunnemann B, Plumpton C, Merlo Pich E, Terstappen G. 2001. Distribution of the messenger RNA for the small conductance calcium-activated potassium channel SK3 in the adult rat brain and correlation with immunoreactivity. *Neuroscience* 102: 209-15

Takeda H, Shimada A. 2010. The art of medaka genetics and genomics: what makes them so unique? *Annual review of genetics* 44: 217-41

Takehana Y. 2006. Molecular phylogeny and sex chromosome evolution of the medaka fishes.

Taranger GL, Carrillo M, Schulz RW, Fontaine P, Zanuy S, Felip A, Weltzien FA, Dufour S, Karlsen Ø, Norberg B. 2010. Control of puberty in farmed fish. *General and comparative endocrinology* 165: 483-515

Tena-Sempere M. 2006. KiSS-1 and reproduction: focus on its role in the metabolic regulation of fertility. *Neuroendocrinology* 83: 275-81

Toro L, Wallner M, Meera P, Tanaka Y. 1998. Maxi-K (Ca), a Unique Member of the Voltage-Gated K Channel Superfamily. *News in physiological sciences: an international journal of physiology produced jointly by the International Union of Physiological Sciences and the American Physiological Society* 13: 112

Trapnell C, Pachter L, Salzberg SL. 2009. TopHat: discovering splice junctions with RNA-Seq. *Bioinformatics* 25: 1105-11

Trapnell C, Roberts A, Goff L, Pertea G, Kim D, Kelley DR, Pimentel H, Salzberg SL, Rinn JL, Pachter L. 2012. Differential gene and transcript expression analysis of RNA-seq experiments with TopHat and Cufflinks. *Nature Protocols* 7: 562-78

Tse A, Hille B. 1992. GnRH-induced Ca2+ oscillations and rhythmic hyperpolarizations of pituitary gonadotropes. *Science* 255: 462

Tsutsui K, Bentley GE, Ubuka T, Saigoh E, Yin H, Osugi T, Inoue K, Chowdhury VS, Ukena K, Ciccone N. 2007. The general and comparative biology of gonadotropin-inhibitory hormone (GnIH). *General and comparative endocrinology* 153: 365-70

Tzur A, Moore JK, Jorgensen P, Shapiro HM, Kirschner MW. 2011. Optimizing optical flow cytometry for cell volume-based sorting and analysis. *PloS one* 6: e16053

Valverde MA, Rojas P, Amigo J, Cosmelli D, Orio P, Bahamonde MI, Mann GE, Vergara C, Latorre R. 1999. Acute activation of Maxi-K channels (hSlo) by estradiol binding to the subunit. *Science's STKE* 285: 1929

Van Aerle R, Kille P, Lange A, Tyler C. 2008. Evidence for the existence of a functional Kiss1/Kiss1 receptor pathway in fish. *Peptides* 29: 57-64

Van Der Kraak G, Suzuki K, Peter RE, Itoh H, Kawauchi H. 1992. Properties of common carp gonadotropin I and gonadotropin II. *General and comparative endocrinology* 85: 217-29

Van Goor F, Goldberg J, Chang J. 1996. Involvement of extracellular sodium in agonist-induced gonadotropin release from goldfish (Carassius auratus) gonadotrophs. *Endocrinology* 137: 2859-71

Van Goor F, Li YX, Stojilkovic SS. 2001. Paradoxical role of large-conductance calcium-activated K+ (BK) channels in controlling action potential-driven Ca2+ entry in anterior pituitary cells. *The Journal of Neuroscience* 21: 5902-15

Vandorpe DH, Shmukler BE, Jiang L, Lim B, Maylie J, Adelman JP, de Franceschi L, Cappellini MD, Brugnara C, Alper SL. 1998. cDNA cloning and functional characterization of the mouse Ca2+-gated K+ channel, mIK1. *Journal of Biological Chemistry* 273: 21542-53

Vergara C, Latorre R, Marrion NV, Adelman JP. 1998. Calcium-activated potassium channels. *Current opinion in neurobiology* 8: 321-29

Vidal B, Pasqualini C, Le Belle N, Holland MCH, Sbaihi M, Vernier P, Zohar Y, Dufour S. 2004. Dopamine inhibits luteinizing hormone synthesis and release in the juvenile European eel: a neuroendocrine lock for the onset of puberty. *Biology of reproduction* 71: 1491-500

Vilella AJ, Severin J, Ureta-Vidal A, Heng L, Durbin R, Birney E. 2009. EnsemblCompara GeneTrees: Complete, duplication-aware phylogenetic trees in vertebrates. *Genome research* 19: 327-35

Wang L, Li P, Brutnell TP. 2010. Exploring plant transcriptomes using ultra high-throughput sequencing. *Briefings in functional genomics* 9: 118-28

Wang Z, Gerstein M, Snyder M. 2009. RNA-Seq: a revolutionary tool for transcriptomics. *Nature Reviews Genetics* 10: 57-63

Waring DW, Turgeon JL. 2009. Ca2+-activated K+ channels in gonadotropin-releasing hormone-stimulated mouse gonadotrophs. *Endocrinology* 150: 2264-72

Wei AD, Gutman GA, Aldrich R, Chandy KG, Grissmer S, Wulff H. 2005. International Union of Pharmacology. LII. Nomenclature and molecular relationships of calcium-activated potassium channels. *Pharmacological reviews* 57: 463-72

Weltzien FA, Andersson E, Andersen Ø, Shalchian-Tabrizi K, Norberg B. 2004. The brain–pituitary–gonad axis in male teleosts, with special emphasis on flatfish (< i> Pleuronectiformes</i>). *Comparative Biochemistry and Physiology-Part A: Molecular & Integrative Physiology* 137: 447-77

Weltzien FA, Norberg B, Swanson P. 2003. Isolation and characterization of FSH and LH from pituitary glands of Atlantic halibut (Hippoglossus hippoglossus L.). *General and comparative endocrinology* 131: 97-105

Wilhelm BT, Landry JR. 2009. RNA-Seq—quantitative measurement of expression through massively parallel RNA-sequencing. *Methods* 48: 249-57

Wurmbach E, Yuen T, Ebersole BJ, Sealfon SC. 2001. Gonadotropin-releasing hormone receptor-coupled gene network organization. *Journal of Biological Chemistry* 276: 47195-201

Xia XM, Fakler B, Rivard A, Wayman G, Johnson-Pais T, Keen J, Ishii T, Hirschberg B, Bond C, Lutsenko S. 1998. Mechanism of calcium gating in small-conductance calcium-activated potassium channels. *Nature* 395: 503-07

Yan J, Olsen JV, Park KS, Li W, Bildl W, Schulte U, Aldrich RW, Fakler B, Trimmer JS. 2008. Profiling the phospho-status of the BKCa channel α subunit in rat brain reveals unexpected patterns and complexity. *Molecular & Cellular Proteomics* 7: 2188-98

Yan L, Swanson P, Dickhoff W. 1992. A two-receptor model for salmon gonadotropins (GTH I and GTH II). *Biology of reproduction* 47: 418-27

Yaron Z, Gur G, Melamed P, Rosenfeld H, Elizur A, Levavi-Sivan B. 2003. Regulation of fish gonadotropins. *International review of cytology* 225: 131-85

Yu K, Rosenblum P, Peter R. 1991. < i> In vitro</i> release of gonadotropin-releasing hormone from the brain preoptic-anterior hypothalamic region and pituitary of female goldfish. *General and comparative endocrinology* 81: 256-67

Yu KL, He ML, Chik CC, Lin XW, Chang JP, Peter RE. 1998. mRNA expression of gonadotropin-releasing hormones (GnRHs) and GnRH receptor in goldfish. *General and comparative endocrinology* 112: 303-11

Zhang H, Bailey JS, Coss D, Lin B, Tsutsumi R, Lawson MA, Mellon PL, Webster NJG. 2006. Activin modulates the transcriptional response of LβT2 cells to gonadotropin-releasing hormone and alters cellular proliferation. *Molecular Endocrinology* 20: 2909-30

Zohar Y, Muñoz-Cueto JA, Elizur A, Kah O. 2010. Neuroendocrinology of reproduction in teleost fish. *General and comparative endocrinology* 165: 438-55

8 Appendix

8.1 Appendix 1

Table 2 Common names, Latin names and reference sequences found in NCBI or Ensembl for the BK channel sequences used in the phylogenetic analysis.

Channel	Gene	Latin name	Common name	Reference sequence
BK	KCNMA1	*Danio rerio*	Zebrafish	NM_001145600.1
BK	KCNMA1	*Homo sapiens*	Human	NM_001161352.1
BK	KCNMA1	*Anolis carolinensis*	Green anole	NW_002198840.1
BK	KCNMA1	*Sus scrofa*	Pig	NM_214219.1
BK	KCNMA1	*Rattus norvegicus*	Norway rat	NM_031828.1
BK	KCNMA1	*Cricetulus griseus*	Chinese hamster	XM_003496744.1
BK	KCNMA1	*Xenopus laevis*	African clawed frog	NM_001085690.1
BK	KCNMA1	*Bos Taurus*	Cattle	NM_174680.2
BK	KCNMA1	*Canis lupus*	Dog	NM_001003300.1
BK	KCNMA1	*Oryzias latipes*	Medaka	ENSORLG00000006622
BK	KCNMA1	*Oryzias latipes*	Medaka	ENSORLG00000008798
BK	KCNMA1	*Gadus morhua*	Cod	ENSGMOG00000000234
BK	KCNMA1	*Gadus morhua*	Cod	ENSGMOG00000012618

Table 3 Common names, Latin names and reference sequences found in NCBI or Ensembl for the SK1 channel sequences used in the phylogenetic analysis.

Channel	Gene	Latin name	Common name	Reference sequence
SK1	KCNN1	*Bos taurus*	Cattle	XM_002688571.2
SK1	KCNN1	*Danio rerio*	Zebrafish	BC153898.1
SK1	KCNN1	*Homo sapiens*	Human	NM_002248.3
SK1	KCNN1	*Macaca mulatta*	Rhesus monkey	XM_001115129.2
SK1	KCNN1	*Mus musculus*	House mouse	NM_032397.2
SK1	KCNN1	*Sus scrofa*	Pig	XM_003123502.1
SK1	KCNN1	*Xenopus tropicalis*	Western clawed frog	NM_001079016.1
SK1	KCNN1	*Danio rerio*	Zebrafish	NM_001045199.2
SK1	KCNN1	*Rattus norvegicus*	Rat	NM_019313.1
SK1	KCNN1(1/2)	*Gadus morhua*	Cod	ENSGMOG00000010301
SK1	KCNN1(2/2)	*Gadus morhua*	Cod	ENSGMOG00000010609
SK1	KCNN1(1/2)	*Oryzias latipes*	Medaka	ENSORLG00000006679
SK1	KCNN1(2/2)	*Oryzias latipes*	Medaka	ENSORLG00000008777

Table 4 Common names, Latin names and reference sequences found in NCBI or Ensembl for the SK2 channel sequences used in the phylogenetic analysis

Channel	Gene	Latin name	Common name	Reference sequence
SK2	KCNN2	*Rattus norvegicus*	Rat	NM_019314.1
SK2	KCNN2	*Mus musculus*	Mouse	NM_080465.2
SK2	KCNN2	*Bos taurus*	Cattle	GJ061947.1
SK2	KCNN2	*Canis lupus*	Dog	XM_844161.2
SK2	KCNN2	*Gadus morhua*	Cod	ENSGMOG00000015908
SK2	KCNN2	*Pongo abelii*	Sumatran orangutan	NM_001131645.1
SK2	KCNN2	*Oryzias latipes*	Medaka	ENSORLG00000009605
SK2	KCNN2	*Xenopus laevis*	African Clawed frog	JN831317.1
SK2	KCNN2	*Gallus gallus*	Chicken	NM_204798.1
SK2	KCNN2	*Danio rerio*	Zebrafish	ENSDARG00000014939
SK2	KCNN2	*Homo sapiens*	Human	NM_021614.2
SK2	KCNN2	*Macaca mulatta*	Rhesus monkey	XM_001084002

Table 5 Common names, Latin names and reference sequences found in NCBI or Ensembl for the SK3 channel sequences used in the phylogenetic analysis

Channel	Gene	Latin name	Common name	Reference sequence
SK3	KCNN3	*Bos taurus*	Cattle	GJ060612.1
SK3	KCNN3	*Rattus norvegicus*	Rat	NM_019315.2
SK3	KCNN3	*Mus musculus*	Mouse	NM_080466.2
SK3	KCNN3	*Sus scrofa*	Pig	NM_213985.1
SK3	KCNN3	*Gadus morhua*	Cod	ENSGMOG00000019038
SK3	KCNN3	*Oryzias latipes*	Medaka	ENSORLG00000009976
SK3	KCNN3	*Homo sapiens*	Human	AY049734.1
SK3	KCNN3	*Canis lupus*	Dog	XM_547563.2
SK3	KCNN3	*Danio rerio*	Zebrafish	XM_001921759.2

Table 6 Common names, Latin name and reference sequences found in NCBI or Ensembl for the IK channel sequences used in the phylogenetic analysis

Channel	Gene	Latin name	Common name	Reference sequence
IK	KCNN4	*Bos taurus*	Cattle	GJ062555.1
IK	KCNN4	*Rattus norvegicus*	Rat	NM_023021.1
IK	KCNN4	*Homo sapiens*	Human	NM_002250.2
IK	KCNN4	*Cavia porcellus*	Domestic guinea pig	NM_001173122.1
IK	KCNN4	*Mus musculus*	Mouse	NM_001163510.1
IK	KCNN4	*Callithrix jacchus*	White-tufted-ear marmoset	XM_002762276.1
IK	KCNN4	*Danio rerio*	Zebrafish	ENSDARG00000074643
IK	KCNN4	*Danio rerio*	Zebrafish	ENSDARG00000086091
IK	KCNN4	*Gadus morhua*	Cod	ENSGMOG00000004058
IK	KCNN4	*Oryzias latipes*	Medaka	ENSORLG00000006347